Effects of fluctuating hypoxia on benthic oxygen consumption in the Black Sea (Crimean Shelf)

A. Lichtschlag[1, +], D. Donis[1, ++], F. Janssen[1, 2], G. L. Jessen[1], M. Holtappels[1, 3], F. Wenzhöfer[1, 2], S. Mazlumyan[4,+++], N. Sergeeva[4,++++], C. Waldmann[3], A. Boetius[1, 2]

[1] {Max Planck Institute for Marine Microbiology, Celsiusstrasse 1, 28359 Bremen, Germany}

[2] {HGF MPG Research Group for Deep Sea Ecology and Technology, Alfred Wegener Institute for Polar and Marine Research, Am Handelshafen, 27515 Bremerhaven, Germany}

[3] {MARUM – Center for Marine Environmental Sciences, University of Bremen, 28334 Bremen, Germany}

[4] {A.O. Kovalevsky Institute of Biology of Southern Seas, 2, Nakhimov ave., Sevastopol, 299011}

[+] current address: National Oceanography Center, University of Southampton Waterfront Campus, European Way, SO14 3ZH, Southampton, UK}

[++] current address: F.-A. Forel Institute, University of Geneva, Batelle, Bat. D, 7 Route de Drize- 1227 Carouge, Geneva, Switzerland}

[+++] current address: Institute of Natural & Technical Systems Russian Academy of Sciences, Lenin St.28, Sevastopol, 29901, xn--h1aogd.xn--p1ai

[++++] current address: The A.O. Kovalevsky Institute of Marine Biological Research of RAS, 119000, Moscow, Leninsky Ave., 32, imbr.iuf.net

Correspondence to: Anna Lichtschlag (alic@noc.ac.uk)**)**

Abstract

The outer Western Crimean Shelf of the Black Sea is a natural laboratory to investigate effects of stable oxic versus varying hypoxic conditions on seafloor biogeochemical processes and benthic community structure. Bottom-water oxygen concentrations ranged from normoxic (175 µmol O_2 L^{-1}) and hypoxic (< 63 µmol O_2 L^{-1}) or even anoxic/sulfidic conditions within a few kilometres distance. Variations in oxygen concentrations between 160 and 10 µmol L^{-1}

even occurred within hours close to the chemocline at 134 m water depth. Total oxygen uptake, including diffusive as well as fauna-mediated oxygen consumption, decreased from on average 15 mmol m^{-2} d^{-1} in the oxic zone to on average 7 mmol m^{-2} d^{-1} in the hypoxic zone, correlating with changes in macrobenthos composition. Benthic diffusive oxygen uptake rates, comprising respiration of microorganisms and small meiofauna, were similar in oxic and hypoxic zones (on average 4.5 mmol m^{-2} d^{-1}), but declined to 1.3 mmol m^{-2} d^{-1} in bottom waters with oxygen concentrations below 20 µmol L^{-1}. Measurements and modelling of pore-water profiles indicated that reoxidation of reduced compounds played only a minor role in diffusive oxygen uptake under the different oxygen conditions, leaving the major fraction to aerobic degradation of organic carbon. Remineralization efficiency decreased from nearly 100% in the oxic zone, to 50 % in the oxic-hypoxic, to 10 % in the hypoxic-anoxic zone. Overall the faunal remineralization rate was more important, but also more influenced by fluctuating oxygen concentrations, than microbial and geochemical oxidation processes.

1 Introduction

Hypoxia describes a state of aquatic ecosystems in which low oxygen concentrations affect the physiology, composition and abundance of fauna, consequently altering ecosystem functions including biogeochemical processes and sediment-water exchange rates (Middelburg and Levin, 2009). Low faunal bioturbation rates in hypoxic zones limit sediment ventilation (Glud, 2008), decreasing oxygen availability for aerobic respiration. Hence, sediments underlying a low-oxygen water column often show oxygen penetration depths of only a few millimeters (Archer and Devol, 1992; Glud et al., 2003; Rasmussen and Jørgensen, 1992). This increases the contribution of anaerobic microbial metabolism to organic matter remineralization at the expense of aerobic degradation by microbes and fauna as reported from the Romanian Shelf area of the Black Sea (Thamdrup et al., 2000; Weber et al., 2001), the Neuse River Estuary (Baird et al., 2004), and the Kattegat (Pearson and Rosenberg, 1992). Consequently, oxygen is channeled into the reoxidation of reduced substances produced during anaerobic degradation of organic matter and lost for direct aerobic respiration. Even temporarily reduced bottom-water oxygen concentrations can repress seafloor oxygen uptake that should become enhanced by algae blooms and temperature increases (Rasmussen and Jørgensen, 1992). However, depending on frequency and duration of oxygen oscillations, oxygen consumption following an anoxic event can also be significantly increased (Abril et

al., 2010). Hence, these and other studies have indicated, that not only the degree of oxygenation plays an important role in oxygen uptake, but also the frequency and persistency of the low oxygen conditions can shape faunal activity, biogeochemical processes, and the functioning of the ecosystem as a whole (Boesch and Rabalais, 1991, Diaz, 2001, Friedrich et al., 2014).

The outer Western Crimean Shelf of the Black Sea is a natural laboratory where long-term effects of different, and locally fluctuating oxygen concentrations on benthic oxygen consumption and biogeochemical processes can be investigated, which was the main aim of this study. In the Black Sea, the depth of the oxic-anoxic interface changes from about 70-100 m in open waters (Friedrich et al., 2014) to depths of > 150 m above the shelf break (Stanev et al., 2013). This interface is stabilized by a halocline that separates the upper layer of brackish, oxic water (salinity < 17) from the saline, anoxic and sulfidic deep waters below (Tolmazin, 1985). Due to mixing processes by internal waves and eddies, the location of this interface zone is more dynamic along the margins of the Black Sea compared to the open sea. In the shelf region, hypoxic waters with oxygen concentrations < 63 μmol L^{-1} oscillate over > 70 m in water depth on time scales of hours to months (Stanev et al., 2013). On the outer Western Crimean Shelf, such strong vertical fluctuations affect a 40 km wide area of the slope (Friedrich et al., 2014; Luth et al., 1998). Consequences of fluctuating hypoxia on benthic community structure is known from other areas on the Black Sea shelf with seasonally hypoxic coastal areas with water stagnation and high organic carbon accumulation (Zaika et al., 2011).

Here we investigated biogeochemical processes on the outer Western Crimean Shelf to assess how different ranges of oxygen availability, and also of fluctuations in bottom-water oxygen concentrations, influence respiration, organic matter remineralization and the distribution of benthic organisms. The questions addressed are to what extent the variability in oxygen concentration has an effect on (1) the remineralization rates, (2) the proportion of microbial vs. fauna-mediated respiration, (3) the community structure and (4) the share of anaerobic vs. aerobic microbial respiration pathways.

2 Methods

2.1 Study site on the outer Western Crimean Shelf

Investigations of bottom-water oxygen concentrations and biogeochemistry of the underlying seafloor of the outer Western Crimean Shelf were carried out over a time period of 2 weeks (20th April - 7th May 2010) during leg MSM 15/1 of R/V Maria S. Merian. The selected area on the outer shelf has a gentle slope and a maximum width of around 60 km until the shelf break at approx. 200 m water depth. The sediment and the water column were sampled along a transect from 95 m to 218 m water depth within an area of about 100 km^2 (Fig. 1). Detailed information of all stations in the working area is given in Table 1. All biogeochemical data are deposited in the Earth System database www.PANGAEA.de and are available at http://dx.doi.org/10.1594/PANGAEA.844879.

2.2 Water-column CTD and oxygen measurements

Bottom-water oxygen concentrations were recorded repeatedly between 95 m to 218 m water depth at different spatial and temporal scales with various sensors, which were all calibrated by Winkler titration (Winkler, 1888). A total of 26 casts were performed with a CTD/Rosette equipped with a SBE 43 oxygen sensor (Seabird Electronics, Bellevue, WA, USA). A mooring was deployed at 135 m water depth 1.5 m above the sediment, equipped with a Seaguard current meter with CTD and a type 4330 oxygen optode (Aanderaa Data Instruments, Bergen, Norway) recording at 60 seconds intervals at a distance of 1.5 m above the sediment from the 30th April to the 7th May 2010. A second mooring was deployed for the same time period at 100 m water depth, with a CTD attached at 1.5 meter above the sediment (type SBE 16, Seabird Electronics) to record density, salinity and temperature. CTD water-column casts and the mooring at 135 m showed that oxygen concentrations strongly correlate with density (R^2 =0.997). Hence, oxygen concentrations at the 100 m mooring site were calculated from the density recordings at this site using a density-oxygen relationship (4th order polynomial fit) based on the compiled mooring/CTD data. Additionally, bottom-water oxygen concentration was measured at the seafloor by oxygen optodes mounted on the manned submersible JAGO (GEOMAR, Kiel; Aanderaa optode type 3830), and to a Benthic Boundary Layer-Profiler (Holtappels et al., 2011) (Aanderaa optode type 4330). Furthermore, microprofilers equipped with oxygen microsensors were mounted on a lander and a crawler (see 2.5.1). For consistency with other hypoxia studies, we use the oxygen threshold of 63 µmol L^{-1} as upper boundary for hypoxia (Diaz, 2001). Sulfide concentrations were determined in bottom water collected with Niskin bottles during CTD casts and JAGO dives at 13

different locations between 135 m and 218 m water depth. For all water-column oxygen and sulfide concentrations a limit of 2 µmol L^{-1} was defined, below which concentrations were assumed to be zero.

2.3 Visual seafloor observations and micro-topography scans

To observe organisms, their traces of life, and the resulting micro-topography at the surface of the different seafloor habitats, a laser scanning device (LS) and the high-resolution camera MEGACAM were used on the benthic crawler MOVE (MARUM, Bremen). The LS consisted of a linear drive that moved a downward looking line laser together with a monochrome digital camera horizontally along a 700 mm long stretch of the seafloor. The position of the approx. 200 mm wide laser line was recorded by the camera from an angle of 45º and the 3-D micro-topography of the scanned area was determined on a 1 x 1 mm^2 horizontal grid at sub-mm accuracy (for a detailed description see Cook et al., 2007). The roughness of the sediment surface was quantified in three 700 mm long profiles extracted from the sides and along the center line of 7, 2, 6, and 2 micro-topographies scanned at 104, 138, 155, and 206 m water depth, respectively. Roughness was determined for different length scales by calculating mean absolute vertical differences to the same profile previously smoothed by applying moving average with 3 to 300 mm averaging window size.

The downward-looking MEGACAM (Canon EOS T1i with 15 megapixel imager and 20 mm wide-angle lens) was either attached directly to MOVE or added to the horizontal drive of the LS; the latter configuration facilitating imaging of larger sediment stretches by photo-mosaicking. In addition, visual seafloor observations were carried out before pushcore sampling by JAGO. Dive videos were recorded with a type HVR-V1E HDV Camcorder (SONY, Tokyo, Japan) mounted in the center of JAGO's large front viewport during 19 dives. During each dive, video still images were captured by video-grabber from the running camera.

2.4 Faunal analyses

Meiofauna organisms were studied in the upper 5 cm sediment horizons of 2-4 cores per station, with each core covering an area of 70.9 cm^2 (TVMUC) and 41.8 cm^2 (for JAGO pushcore) (Table 1, Fig. 1). The abundances were extrapolated to m^2. Sediments were washed with filtered or distilled water through sieves with mesh sizes of 1 mm and 63 µm, and preserved in 75 % alcohol to conserve the morphological structures of the meiofauna. Subsequently, samples were stained with Rose Bengal, to separate living and dead / decaying

organisms (Grego et al., 2013), and sorted in water using a binocular (x 90 magnification) and a microscope (Olympus CX41 using different magnifications up to x 1000). Only organisms that strongly stained with Rose Bengal and showed no signs of morphological damage were considered as being alive at the time of sampling. All of the isolated organisms were counted and identified to higher taxa. In the same cores we analyzed fauna that are larger than 1.5-2.0 mm and that from their size are representatives of macrobenthos. Also this share of fauna was identified to higher taxa under the microscope, counted and the abundances extrapolated to m^2. Statistical analyses of the similarity of meiofauna communities were conducted using the R package vegan (Oksanen et al., 2010) and performed in R (v. 3.0.1; http://www.R-project.org). Richness was calculated from species (taxa) presence/absence. A matrix based on Bray-Curtis dissimilarities was constructed from the Hellinger-transformed abundances for meiofauna taxa. The non-parametric Analysis of Similarity (ANOSIM) was carried out to test whether the communities (based on different bottom-oxygen zones) were significantly different (Clarke 1993).

2.5 Benthic exchange rates

2.5.1 In situ microsensor measurements

Vertical solute distributions were measured in situ at high resolution in sediment pore waters and the overlying waters with microsensors mounted on microprofiler units (Boetius and Wenzhöfer, 2009). In particular, Clark-type O_2 microsensors (Revsbech, 1989) and H_2S microsensors (Jeroschewski et al., 1996) were used as well as microsensors for pH - either LIX-type (de Beer et al., 1997) or needle-type (type MI 408, Microelectrodes Inc., Bedford, NH, USA). A two-point oxygen sensor calibration was done in situ, using water-column oxygen concentrations obtained from simultaneous oxygen recordings and zero readings in anoxic sediment layers. The H_2S sensors were calibrated at in situ temperature on board at stepwise increasing H_2S concentrations by adding aliquots of a 0.1 mol L^{-1} Na_2S solution to acidified seawater (pH <2). pH was determined as pH_{NBS} with sensors that were calibrated with commercial laboratory buffers and corrected with pH obtained from water samples taken with Niskin bottles operated by JAGO.

Profiler units were mounted either on the benthic crawler MOVE (Waldmann and Bergenthal, 2010) or on a benthic lander (Wenzhöfer and Glud, 2002). The MOVE vehicle was connected to the ship via a fiber optic cable that allowed continuous access to video and sensor data. The maneuverability of the vehicle allowed targeting spots of interest on the seafloor in the cm

range. The profiler units were equipped with 3-4 O_2 microsensors, 2 H_2S microsensors, and 1-2 pH sensors. Microprofiles across the sediment-water interface were performed at a vertical resolution of 100 µm and had a total length of up to 18 cm. During each deployment of the lander the microsensor array performed up to three sets of vertical profiles at different horizontal positions, each 26 cm apart.

From the obtained oxygen profiles the diffusive oxygen uptake (DOU) was calculated based on the gradients in the diffusive boundary layer (DBL) according to Fick's first law of diffusion,

$$J = \frac{dc}{dx} \times D_0 \qquad (1)$$

where J is the oxygen flux, dc/dx is the concentration gradient, and D_0 is the diffusion coefficient of oxygen in water (D_0O_2 = 1.22 x 10^{-4} m^2 d^{-1}, Broecker and Peng (1974)) at the ambient temperature (8 °C) and salinity (18-20). For each station, selected oxygen profiles were fitted using the software PROFILE (Berg et al., 1998) to determine oxygen consumption from the shape of the pore-water gradient and to identify depth intervals of similar oxygen consumption based on statistical F-testing.

2.5.2 In situ benthic chamber incubations

Total oxygen uptake (TOU) of sediments was measured by in situ benthic chamber incubations using 2 platforms: (1) Two benthic chambers, each integrating an area of 0.2 × 0.2 m (Witte and Pfannkuche, 2000) mounted to the same benthic lander frame used for microprofiler measurements (Wenzhöfer and Glud, 2002) and (2) a circular chamber (r = 0.095 m, area = 0.029 m^2) attached to the benthic crawler MOVE for video-guided chamber incubations. After positioning MOVE at the target area the chamber was lowered into the sediment, controlled by the video camera of MOVE and operated online through the MOVE-electronics. Both systems were equipped with a stirrer and syringe samplers that took up to 6 successive samples (V = 50 mL) from the 0.1-0.15 m high overlying bottom water. Benthic exchange rates were determined from the linear regression of oxygen solute concentration over time inside the enclosed water body that was continuously monitored for a period of 2 to 4 h by 1 or 2 oxygen optodes mounted in the chamber lid. The optodes were calibrated with a zero reading at in situ temperature on board and with bottom-water samples, in which concentrations were determined either by Winkler titration (Winkler, 1888) or with a calibrated Aanderaa optode attached to the outside of the chamber. At the beginning of the incubation period, oxygen concentrations in the chamber were the same as in situ bottom-

water concentrations outside the chamber. Only during deployments in the hypoxic-anoxic zone, oxygen concentrations in the chambers were higher than in the surrounding bottom water, due to enclosure of oxygen-rich water during descent. These measurements were used to estimate potential TOU rates at intermittently higher oxygen concentration. To estimate the in situ TOU/DOU ratio for the hypoxic-anoxic zone, in this case we modeled the DOU at these specific conditions based on the volumetric rate and the DBL thickness determined by the in situ microsensor profile.

2.6 Geochemical analyses of the sediments and sulfate reduction rates

Sediments for geochemical analyses were sampled with a video-guided multicorer (TVMUC) at 4 stations between 104 and 207 m (Table 1). Pore water was extracted from sediment cores within 3 h after retrieval in 1 cm (upper 5 cm) or 2 cm (> 5 cm) intervals with Rhizons (type: CSS, Rhizosphere Research Products, pore size < 0.2 µm, length 5 cm) at in situ temperature (8 °C) in a temperature-controlled room. To extract sufficient amounts of pore water two Rhizones were inserted horizontally at each depth interval in holes that were drilled at the same depth, with a 90º angle. Using this procedure, the amount of pore water removed per Rhizon was less than 4 mL and mixing of pore water across the different horizons was avoided (Seeberg-Elverfeldt et al., 2005). Samples were fixed for Fe (II), Mn (II), sulfide and sulfate analyses as described in Lichtschlag et al. (2010). For ammonium and nitrate analyses samples were frozen at -20 °C. In addition, one sediment core from each station was sliced in 1 cm intervals (upper 10 cm) and 2 cm intervals (>10 cm depth) for solid phase analyses. Aliquots were stored at 4 °C for porosity analyses and frozen at -20 °C for ^{210}Pb and solid phase iron, manganese and elemental sulfur analyses.

Pore-water constituents were analyzed by the following procedures: Dissolved Mn (II) and Fe (II) were measured with a Perkin Elmer 3110 flame atomic absorption spectrophotometer (AAS) with a detection limit of 5 µmol L^{-1} for iron and manganese. Total sulfide concentrations ($H_2S + HS^- + S^{2-}$) were determined with the diamine complexation method (Cline, 1969). A Skalar Continuous-Flow Analyzer was used for ammonium and nitrate analyses following the procedures described in Grasshoff (1983), with a detection limit of 1 µmol L^{-1}. Sulfate concentrations in pore water were determined by non-suppressed anion exchange chromatography (Metrohm 761 Compact IC) after filtration and dilution. To determine fluxes of iron, manganese, sulfide and ammonium the pore-water profiles were fitted using the software PROFILE (Berg et al., 1998).

Total zero-valent sulfur in sediments was extracted with methanol from sediment preserved in ZnAc (Zopfi et al., 2004) and analyzed by HPLC. Concentrations of acid volatile sulfide (AVS = Fe_3S_4, FeS) and chromium reducible sulfur (CRS = FeS_2, some S^0, remaining Fe_3S_4) were determined on frozen sediment aliquots by the two-step Cr-II distillation method (Fossing and Jørgensen, 1989). Solid phase reactive iron and manganese were extracted from frozen sediments after the procedure of Poulton and Canfield (2005) using sequentially Na-acetate, hydoxylamine-HCl, dithionite and oxalate. Manganese and iron concentrations were measured as described above. Organic carbon content in the first cm of the sediments was determined on freeze-dried and homogenized samples and measured using a Fisons NA-1500 elemental analyzer.

Sulfate reduction rates were determined with the whole core incubation method described in Jørgensen (1978). On board 10 µL aliquots of an aqueous $^{35}SO_4^{2-}$ tracer solution (activity 11.5 kBq μL^{-1}) were injected into the sediments in 1 cm intervals and samples were incubated for up to 24 h at in situ temperature, until the sediments were sliced into 20 mL 20 % ZnAc. Tracer turnover rates were determined with the single-step cold distillation method (Kallmeyer et al., 2004). Three replicates were measured per station and results were integrated over the upper 10 cm of the sediment.

Porosity and solid-phase density were determined by drying a wet sediment aliquot of known volume at 105 °C until constant weight and weighing before and after.

Sediment accumulation rates were determined from excess ^{210}Pb activity ($^{210}Pb_{xs}$) in frozen sediment aliquots of the upper 10 cm that were freeze-dried and homogenized by grinding. Activities of ^{210}Pb, ^{214}Pb and ^{214}Bi were determined on 5-30 g aliquots by non-destructive gamma spectrometry using an ultra-low-level germanium gamma detector (EURISYS coaxial type N, Canberra Industries, Meriden, CT, U.S.A.). Sediment accumulation rates (g cm^{-2} yr^{-1}) were calculated from the undisturbed part of the sediments from the change of the unsupported $^{210}Pb_{xs}$ activity with sediment accumulation, expressed as cumulative dry weight (g cm^{-2}) and using the calculations described by Niggemann et al. (2007). This calculation is based on the assumption that the $^{210}Pb_{xs}$ flux and sediment accumulation were constant over time.

3 Results

3.1 Oxygen regime of the outer Western Crimean Shelf

Recordings of bottom-water oxygen concentrations (n=85) along the transect from 95 m to 218 m water depth served to differentiate four zones of different bottom-water oxygenation within a distance of more than 30 km (Table 1; Fig. 1; Fig. 2):

The "oxic zone" at water depths of 95 to 130 m had oxygen concentrations of on average 116 ±29 μmol L^{-1} (31 % air saturation at ambient conditions; 8 °C, salinity of 19), and remained above the threshold for hypoxia (63 μmol L^{-1}) throughout the period of our observations. Recordings from the mooring at 100 m water depth showed some fluctuations (Fig. S1a in the Supplement), with oxygen concentrations varying between 100 - 160 μmol L^{-1} within 6 days. In this oxic zone, sediment surface color was brownish, and the seafloor looked rather homogenous, without ripple structures, but with faunal traces (Fig. S2a). The top 5 cm of the sediment comprised some shell debris of 2 - 6 mm diameter encrusted with a bright orange layer of up to 3 mm thickness, which most probably consisted of iron-oxides (Fig. S2b). During JAGO dives and MOVE deployments we recorded living fauna in the oxic zone such as clams, ascidians, phoronids, cerianthids, porifera and many fish (Fig. S2c). Traces of recent faunal activity at the seafloor included trails, worm borrows and feces (Fig. S2a). During our sampling campaign the horizontal distance to the oxic-anoxic interface (chemocline) was on average 13 km. The oxic zone served as reference for further comparisons of hypoxic effects on biogeochemical processes and faunal community composition.

In the "oxic-hypoxic zone" at water depths between 130 m to 142 m, average bottom-water oxygen concentrations were 94 ±56 μmol L^{-1} (approx. 25 % air saturation at ambient conditions; 8 °C, salinity of 20). However, we observed strong variations in oxygen concentrations with maxima of up to 176 μmol L^{-1} and minima of 9 μmol L^{-1}, respectively. Hypoxic conditions prevailed for 30 % of the observation period of 7 days, as recorded by the stationary mooring at 135 m water depth (Fig. S1b). Constantly rising oxygen concentrations over days were interspersed by a substantial drop from fully oxic to almost anoxic conditions within < 3 h (Fig. S1b). Horizontal distance to the oxic-anoxic interface was on average 7 km during our expedition. In the oxic-hypoxic zone, only few fishes were observed, and video-observations of the seafloor showed a clear reduction of epibenthos abundance and their traces compared to those in the oxic zone.

The "hypoxic-anoxic" zone between 142 and 167 m water depth sediments showed fluctuating hypoxic conditions between 0 - 63 µmol L^{-1} (average 11 ±16 µmol L^{-1}; 3 % air saturation at ambient conditions; 8 °C, salinity of 20). Unexpectedly, during a short period at these water depths, some fish (the sprattus *Sprattus phalericus* at 145 and 163 m water depth, and the whiting *Merlangius merlangus euxinus* at 145 m water depth, Zaika and Gulin (2011)) were observed when oxygen concentrations were as low as 20 µmol L^{-1} (Fig. S2f). The seafloor was covered with fluffy greenish-brownish material and sediments showed a fine lamination (Fig. S2e). No epibenthic life was observed, nor borrows or other traces of bottom dwelling fauna.

Below 167 m, the bottom water was permanently anoxic during the time period of our campaign. Below 180 m sulfide was constantly present in the bottom water, with concentrations ranging between 5-23 µmol L^{-1} (Fig. 2). In this "anoxic-sulfidic" zone sediments were dark green-blackish. Neither macrofauna, nor traces of bottom-dwelling infauna were observed.

3.2 Meiofauna composition and abundance

Abundance and composition of macro- and meiobenthos as retrieved from the top 5 cm of pooled core samples were compared across the different zones of oxygen availability indicated in Figure 2 (Table S1 and S2 in the Supplement). The macrobenthos abundances and taxonomic composition presented here are not quantitative, nor statistically significant, for the entire size class due to the limited sample size available; they might represent mostly small types and juvenile stages (Table S1 in the Supplement). These decreased by more than one order of magnitude from the oxic zone (21 $x10^3$ individuals m^{-2}) to the hypoxic-anoxic zone (1 $x10^3$ individuals m^{-2}) (Table S1). In the oxic zone, cnidaria dominated the benthic community next to oligochaetes and polychaetes, also bivalves and gastropods were present. A peak in macrobenthos abundances in both the oxic and the oxic-hypoxic zone at around 129-138 m was related to an accumulation of cnidarians with abundances of up to 54 $x10^3$ individuals m^{-2} (Table S1). Also the two hypoxic zones were dominated by cnidaria. In accordance with the results from sampling, no larger macrofauna was documented during JAGO dives in these zones.

Meiobenthos was composed of similar groups and abundances in the oxic and oxic-hypoxic zone with densities of around 200 $x10^4$ individuals m^{-2} (Fig. 3, Table S2). A substantial decrease to 50 $x10^4$ individuals m^{-2} was observed between these two zones and the hypoxic-

anoxic zone. The meiofaunal community structure changed according to the oxygenation regime (Fig. 4), showing significant differences between oxic and hypoxic-anoxic zones (ANOSIM-R = 0.7, Bonferroni corrected P value < 0.05) together with the highest dissimilarities (up to 50%, Table S3). Nematodes dominated meiofauna composition in all oxic and hypoxic zones (Table S2). In the oxic zone ostracodes were the 2nd most abundant species. These were replaced by benthic foraminifera in the oxic-hypoxic and the hypoxic-anoxic zone. Altogether meiofaunal richness (taxa count, average ±SD) was similar in the oxic zone and oxic-hypoxic zone (15 ±2 and 15 ±1) and dropped to 9 ±1 in the hypoxic-anoxic zone.

3.3 Benthic oxygen fluxes and respiration rates

A total of 33 oxygen microprofiles were measured during seven deployments of the benthic crawler MOVE and the lander at water depths between 104 and 155 m. Oxygen penetration depths and dissolved oxygen uptake rates are summarized in Table 2. The shape of the profiles and the differences in oxygen penetration depth as shown in Figure 5 reflect the spatial variations of oxygen bottom-water concentrations and oxygen consumption rates. In the shallowest, oxic zone (104 m) clear signs of bioturbation were visible from the irregular shape of about 25 % of the profiles, occasionally increasing the oxygen penetration depth up to approximately 10 mm. Bioturbation activity was in accordance with a significant bioturbated surface layer and more pronounced roughness elements at the sediment surface at the shallowest site as compared to deeper waters (see section 3.5). In contrast, the shape of the oxygen profiles obtained in the oxic-hypoxic and the hypoxic-anoxic zone showed no signs of bioturbation. Small-scale spatial heterogeneity was low between parallel sensor measurements and within one deployment (area of 176 cm^2 sampled). However, strong temporal variations occurred in response to the fluctuations in bottom-water oxygen concentration. For example, in the oxic-hypoxic zone a clear relation between oxygen penetration depth and bottom-water oxygen concentration was detectable, with increased bottom-water oxygen concentration leading to deeper oxygen penetration depth (Fig. 5 a-c). Except where bioturbation led to slightly deeper penetration, oxygen was depleted within the first 0.4-3 mm of the surface layer (Fig. 5, Table 2).

Diffusive oxygen uptake (DOU) ranged within an order of magnitude between all zones (Table 2). The highest DOU of 8.1 mmol m^{-2} d^{-1} was calculated from a profile obtained at 104 m water depth in the oxic zone, but the averages of all oxygen fluxes measured in the oxic and

oxic-hypoxic zones were similar (averages ±SD of 4.6 ±1.8 mmol m^{-2} d^{-1} and 4.4 ±1.9, respectively, Table 2). The higher variability within the oxic-hypoxic zone, spanning from 0.6 to 8 mmol m^{-2} d^{-1} between measurements, matches the higher variability in bottom-water oxygen concentrations observed for this zone (Fig. 4b). Diffusive oxygen uptake in that zone was lowest after a nearly anoxic event (~10 µmol O_2 L^{-1}; Fig. S1b). However, highest fluxes in the oxic-hypoxic zone were not recorded during a "normoxic event" (144 µmol O_2 L^{-1}, Fig. 6b), but at the typical intermediate bottom-water oxygen concentration of approx. 80 µmol L^{-1} (Station 434; Fig. 6c, Fig. S1b). In the hypoxic-anoxic zone DOU was only 25% of that in the oxic and oxic-hypoxic zones (average: 1.3 ±0.5 mmol m^{-2} d^{-1}).

In bottom waters of the hypoxic-anoxic zone high resolution measurements of pH indicated a pH_{NBS} of around 7.8, decreasing to values between 7.2 - 7.4 in the sediment. With the H_2S microsensors no free sulfide was detected in the pore waters of the oxic, oxic-hypoxic or hypoxic-anoxic zones down to the measured depth of 15 cm in the sediment. In the anoxic-sulfidic zone the microsensor measurements failed. Bottom-water sulfide concentrations were > 5 µmol L^{-1}, and the pore-water analyses indicated high concentrations of sulfide of up to 1000 µmol L^{-1} in the sediment (see 3.4).

Total oxygen uptake (TOU) including the faunal respiration, was generally higher than DOU (Table 2). Individual measurements varied from 20.6 to 3.2 mmol m^{-2} d^{-1} across all zones. Average TOU showed a clear reduction from the oxic zone (average: 14.9 ±5.1 mmol m^{-2} d^{-1}) to the oxic-hypoxic zone (average: 7.3 ±3.5 mmol m^{-2} d^{-1}). TOU at the oxic-hypoxic station compare well with a TOU of 6.0 and 4.2 mmol m^{-2} d^{-1} determined by simultaneous eddy correlation measurements averaged over a time period of 14 hours (Holtappels et al., 2013).

Trapping of oxygen-enriched waters in the chambers during deployments carried out at the hypoxic-anoxic zone led to higher initial oxygen concentrations in the enclosed water as compared to ambient bottom waters. Therefore, we could only obtain potential TOU rates at elevated bottom-water oxygen concentrations of 70 µmol L^{-1}. A potential TOU of 7 mmol m^{-2} d^{-1} was measured and a potential DOU of 5.6 ±0.5 was modeled from the volumetric rates and DBL thickness obtained by the microsensor profiles. The contribution of DOU was lowest in the oxic zone (30%), and increased with decreasing TOU towards the oxic-hypoxic (60%) and hypoxic-anoxic zone (80%) (Table 2).

3.4 Sediment geochemistry

Cores from all sites had the typical vertical zonation of modern Black Sea sediments with a brown/black fluffy layer (oxic and hypoxic zones, Fig. S2d), or dark/grey fluffy layer (anoxic-sulfidic zone), covering beige-grey, homogenous, fine-grained mud. Substantial differences in the concentration profiles and volumetric production and consumption rates of dissolved iron, dissolved manganese, sulfide, and ammonium were found in pore waters from surface sediments sampled from the four different oxygen regimes (Fig. 7). In the oxic zone, dissolved iron and manganese were present in the pore water with maximal concentrations of 217 µmol L^{-1} (Fig. 7a) and 30 µmol L^{-1} (Fig. 7b), respectively, and no free sulfide was detected (Fig. 7c). In the oxic-hypoxic zone, concentrations of dissolved iron were reduced (max. 89 µmol L^{-1}, Fig. 7h), manganese concentrations were below detection (Fig. 7i), but free sulfide was still not present in the pore waters (Fig. 7j). In the hypoxic-anoxic zone dissolved iron and sulfide concentrations were below or close to detection limit (Fig. 7o, q), and some dissolved manganese was present in the lower part of the sediment (Fig. 7p). The station in the anoxic-sulfidic zone had no dissolved iron and manganese, but pore-water concentrations of sulfide increased to up to 1000 µmol L^{-1} at 30 cm sediment depth (Fig. 7v-x). Nitrate concentrations were 1 µmol L^{-1} in the first centimeter of the sediment in the oxic and the oxic-hypoxic zone and dropped below detection limit in the deeper sections. Nitrate was not detected in the sediments of the hypoxic-anoxic or the anoxic-sulfidic zone (data not shown). Ammonium concentrations increased with increasing sediment depth in the top few cm of sediments sampled from the oxic to hypoxic zone (0-100 µmol L^{-1}) and the anoxic-sulfidic zone (0-300 µmol L^{-1}), but rates of ammonium production upon organic carbon degradation were generally low (< 0.6 mmol m^{-3} d^{-1}, Fig. 7d, k, r, y).

In solid phase extractions, reactive iron was elevated in the 0-1 cm interval of the oxic zone and iron oxides were present throughout the upper 30 cm of surface sediments (Fig. 7e). In contrast, concentrations of iron-oxides in the upper 10 cm of the oxic-hypoxic zone were clearly reduced and dropped to background concentrations below 10 cm. The same trend was observed in sediments of the hypoxic-anoxic and the anoxic-sulfidic zone (Fig. 7l, s, z). Solid phase manganese concentration was only clearly elevated in the 0-1 cm interval of the oxic zone (Fig. 7f) and at or close to background concentration below 1 cm, as in all other zones (Fig. 7m, t, aa).

Although pore-water concentrations of sulfide were below detection limit in the oxic to hypoxic-anoxic zones, the presence of reduced solid sulfide phases (AVS, CRS and S^0, Fig. 7g, n, u, ab) and measured sulfate reduction rates indicate that some sulfate reduction took place below the oxygenated sediment. Sulfate reduction rates, integrated over the upper 10 cm of the sediment, represent gross sulfide production and compare well to net sulfide fluxes calculated from the pore-water profiles in Table 3. Altogether, seafloor sulfate reduction rates were increasing nearly 40-fold from <0.1 mmol m^{-2} d^{-1} in the oxic zone to 3.7 mmol m^{-2} d^{-1} in the anoxic-sulfidic zone. In all cores sulfate concentrations were constant with 16 mmol L^{-1} over the upper 30 cm of the sediment (data not shown). Organic carbon content in the first cm of the sediment was lowest in the oxic zone (2.7 ±1.0 % dw), nearly doubled in the oxic-hypoxic zone (4.6 ±0.9 % dw) and highest in the hypoxic-anoxic zone (5.8 ±1.7 % dw), Table 2.

3.5 Sediment accumulation and bioturbation

Sediment porosity was similar across all sites with 0.9 ±0.03 in the top cm and 0.8 ±0.07 averaged over the top 10 cm. Sediment accumulation rates, calculated from the decrease of $^{210}Pb_{xs}$ with depth and cumulative dry weight, varied around 1 ±0.5 mm yr^{-1} for the upper 10 cm of the oxic-hypoxic and the hypoxic-sulfidic zone (Fig. S4). Nearly constant $ln^{210}Pb_{xs}$ values in the upper 2 cm of the oxic zone indicate active sediment mixing by bioturbation. In all other zones, an intensely mixed surface layer was missing and the linear decrease started right below the sediment surface. This is in agreement with reduced sediment mixing in the zones with lower oxygen availability. A stronger bioturbation at the oxic site as compared to the oxic-hypoxic and hypoxic-anoxic site matches the micro-topographies observed at the different sites. Average absolute roughness heights at a water depth of 104 m were generally ~1.8, ~3.2, and ~3.9 times larger than at 138, 155, and 206 m depth, respectively, at all investigated length scales (i.e., averaging windows). At an averaging window of 50 mm, a horizontal scale that covers many biogenic roughness elements, e.g., fecal mounds or funnels of burrows, average absolute deviations from the smoothed surface were 0.42 ±0.16 mm at 104 m, 0.23 ±0.03 mm at 138 m, 0.15 ±0.03 mm at 155 m, and 0.13 ±0.01 mm at 206 m water depth. Figure S3 shows example 3D micro-topographies and extracted profiles (original and smoothed at 155 mm window size).

4 Discussion

4.1 Effect of oxygen availability on remineralization rates and reoxidation processes

Rates of benthic oxygen consumption are governed by a variety of factors including primary production, particle export, quality of organic matter, bottom-water oxygen concentrations, and faunal biomass (Jahnke et al., 1990; Middelburg and Levin, 2009; Wenzhöfer and Glud, 2002). Here we investigated the effects of variable hypoxic conditions, with bottom-water oxygen concentrations ranging from 180-0 μmol L^{-1} within one region of similar productivity and particle flux. On the outer Western Crimean Shelf rapid and frequent variations of oxygen concentrations included strong drops in oxygen concentrations within hours, lasting for up to a few days (Fig. S1b). Such events are likely connected to the special hydrological system of the area, including the strongly variable Sevastopol Eddy (Murray and Yakushev, 2006), that is known to be of importance for the ventilation of the Crimean Shelf (Stanev et al., 2002), possibly in combination with internal waves (Luth et al., 1998; Staneva et al., 2001).

Oxygen consumption in the sediment is usually directly proportional to the total carbon oxidation rate, i.e. carbon oxidized by both aerobic and anaerobic pathways. An imbalance could be the result of denitrification processes, where the reduced product is N_2 gas which is not further involved in sedimentary redox processes, and therefore has no direct bearing on the oxygen budget (Canfield et al., 1993a). Pore-water nitrate concentrations below or close to the detection limit (<1 μmol L^{-1}), suggest that at the time and place of the investigation denitrification might not have been a dominant process in organic carbon degradation. Similarly, the sulfide produced by sulfate reduction could precipitate with dissolved iron without directly consuming oxygen. However solid phase concentrations of iron-solid minerals were generally low, which indicates that sulfide precipitation most likely is not an important pathway for sulfide removal in these sediments. Assuming an annual surface primary productivity of 220 g C m^{-2} yr^{-1}, and a particulate organic carbon (POC) export flux of around 30 % (Grégoire and Friedrich, 2004), about 15 mmol C m^{-2} d^{-1} is expected to reach the seafloor in the investigated area. Based on ocean color satellite data from the studied area, changes in productivity and organic matter flux along the transect are negligible (10 years time frame *MyOcean* data set; http://marine.copernicus.eu/web/69-myocean-interactive-catalogue.php?option=com_csw&view=details&product_id=OCEANCOLOUR_BS_CHL_L3_REP_OBSERVATIONS_009_071; data not shown). With a respiratory quotient of 1 (i.e.,

one mole of oxygen consumed per one mole of CO_2 produced, Canfield et al., 1993a), the average TOU observed in the oxic zone would be sufficient to remineralize nearly all of the organic carbon input to the seafloor (Table 2), with oxygen fluxes measured in this study being similar to those previously reported from the same area (Table 4, including references; Grégoire and Friedrich, 2004). This suggests that within the oxic zone, most deposited carbon is directly remineralized and little carbon is escaping benthic consumption. However, already in the oxic-hypoxic zone, total benthic respiration decreased by 50 %. In the hypoxic-anoxic zone it further decreased to 10%, along with decreases in the abundance and composition of some macrofauna detected in the sediments (Table S1). Accordingly, more organic carbon got preserved in the sediment (Table 2). Through bioturbation and aeration of sediments, macrofauna can enhance total as well as microbially-driven remineralization rates. Hence, absence of macrofauna and low bioturbation activity in areas with temporary hypoxia will affect biogeochemical processes (Levin et al., 2009, and discussion below). In our study area, macrofauna abundance estimates, visual observations, as well as radiotracer and roughness assessments show that already under oxic-hypoxic conditions, sediment aeration by fauna drops rapidly. Consequently, at the onset of hypoxia, substantial amounts of organic matter accumulate in the sediments. Another effect of variable hypoxic conditions on organic matter remineralization rates is the reduced exposure time to oxygen during organic matter degradation (oxygen exposure time: oxygen penetration depth/sediment accumulation rate). At a sediment accumulation rate of 1 mm yr^{-1}, as estimated from ^{210}Pb measurements, particles deposited at the oxic site, are exposed much longer to aerobic mineralization processes (> 5 yr) compared to the other zones (0.4 - 1.6 yr). Earlier studies showed that oxygen availability can be a key factor in the degradability of organic carbon and some compounds such as chlorophyll (King 1995) and amino acids (Vandewiele et al., 2009) will favorably accumulate in the sediments exposed to hypoxic conditions.

To evaluate the contribution of chemical reoxidation to TOU at the outer Western Crimean Shelf, we fitted measured pore-water profiles of dissolved manganese, iron, ammonium, and sulfide with 1-D models to quantify upward directed fluxes (Berg et al., 1998, Table 3, Fig. 7). Taking the stoichiometries of the reaction of oxygen with the reduced species into account, the maximal oxygen demand for the reoxidation of reduced pore-water species was less than 8% (Table 3). This is less than in other studies in eutrophic shelf sediments, where the chemical and microbial reoxidation of reduced compounds, such as sulfide, dominated and

the heterotrophic respiration by fauna contributed around 25 % to total oxygen consumption (Glud, 2008; Heip et al., 1995; Jørgensen, 1982; Konovalov et al., 2007; Soetaert et al., 1996).

4.2 Effect of bottom-water fluctuations on faunal respiration and diffusive oxygen uptake

Comparing total remineralization rates across all zones, including the oxygen demand by anaerobic microbial processes (Table 3), the capacity of the benthic communities to remineralize the incoming particle flux decreased from the oxic zone, to the oxic-hypoxic, hypoxic-anoxic and the anoxic zone. Total remineralization rates were similar in the hypoxic-anoxic and stable anoxic zone, but only in the latter, anaerobic processes dominated, most likely due to the persistent absence of oxygen, allowing anaerobic microbial communities to thrive.

Total oxygen uptake (TOU), as measured in situ with benthic chambers, represents an integrated measure of diffusive microbial respiration, as well as oxygen uptake by benthic fauna. The diffusive oxygen uptake (DOU), as calculated from microsensor profiles, represents mainly aerobic respiration of microorganisms or - although not relevant in our area (see above) - chemical reoxidation (Glud (2008)). In general, the DOU of the outer Western Crimean Shelf sediments was lower than in other shelf zones with seasonally-hypoxic water columns (e.g., Glud et al. 2003), but in the same range as fluxes reported in other Black Sea studies (Table 4). Average DOU was similar in the oxic and oxic-hypoxic zone and only clearly reduced when oxygen concentrations were close to zero (20 μmol L^{-1}). To test if lower fluxes at reduced bottom-water oxygen concentrations rather reflect lowered efficiency of oxygen consumption processes (i.e., rate limitation), or decreased diffusional uptake (i.e., transport limitation), we calculated the highest possible oxygen fluxes theoretically supported by the measured bottom-water oxygen concentration. For this we assumed complete consumption of oxygen at the sediment surface (i.e., oxygen penetration depth approaches zero and volumetric rates approaches infinity), and calculated the flux from measured O_2 concentrations in the bottom water and the observed diffusive boundary layer thickness of 500 μm using Ficks' first law of diffusion (Eq. 1). Maximum theoretical fluxes were 4.3 to 36.4 mmol m^{-2} d^{-1} for the oxic-hypoxic zone and 2.7 to 4.6 mmol m^{-2} d^{-1} for the hypoxic-anoxic zone (for oxygen concentrations see Table 4). Thus, while fluxes are generally not transport limited, the benthic uptake of oxygen approaches its potential maximum when bottom-water oxygenation decreases.

Despite a relatively uniform sediment accumulation rate, TOU at the oxic-hypoxic zone was substantially lower as compared to the oxic zone despite bottom-water oxygen concentrations remained mostly above the common threshold for hypoxia of 63 µmol L^{-1} (Fig. 2, 5). This indicates that total oxygen uptake is more sensitive to varying bottom-water oxygen concentrations than diffusive uptake mediated by microorganisms. To quantify the extent to which benthos-mediated oxygen uptake (BMU) is affected by dynamic oxygen conditions, BMU was calculated from the difference between TOU and DOU (Glud, 2008; Wenzhöfer and Glud, 2004). BMU includes not only oxygen demand of the fauna itself but also oxygen consumption that is related to the increase in oxygen-exposed sediment area due to sediment ventilation and reworking by faunal activity. Based on these calculations we assume that up to 70 % of the total oxygen uptake in the oxic zone, 40 % in the oxic-hypoxic zone and 20% in the hypoxic-anoxic zone is due to benthos-mediated oxygen uptake. The remaining share (30, 60, 80 %, respectively) will mainly be channeled directly into the aerobic degradation of organic carbon by microbes (and potentially also some meiofauna). A BMU of 70 % (10.3 mmol m^{-2} d^{-1}) in the oxic zone was considerably higher than values of 15-60 % reported from shelf sediments underlying both normoxic (Glud et al., 1998; Heip et al., 2001; Moodley et al., 1998; Piepenburg et al., 1995) and hypoxic water columns (Archer and Devol, 1992; Wenzhöfer et al., 2002). A BMU of 40 % in the oxic-hypoxic zone was still well within the ranges of some normoxic water columns (Glud et al., 1998; Heip et al., 2001; Moodley et al., 1998; Piepenburg et al., 1995).

It has previously been shown that sediment-water exchange rates can be altered due to changes in fauna composition in response to different bottom-water oxygenation (Dale et al., 2013; Rossi et al., 2008). Coastal hypoxic zones often show reduced faunal abundances, biodiversity, and loss of habitat diversity below a threshold of 63 µmol O_2 L^{-1} (Diaz, 2001; Levin et al., 2009). In dynamic coastal hypoxic zones with fluctuating conditions as the Kattegat (Diaz, 2001), off the coast of New York/New Jersey (Boesch and Rabalais, 1991), or the Romanian Shelf of the Black Sea (Friedrich et al., 2014), mass mortality has been reported when oxygen concentrations drop below 22 µmol L^{-1} (0.5 ml L^{-1}) (Levin, 2003; Levin et al., 2009). In contrast, in regions under stable low-oxygen conditions faunal communities can be adapted to such physiologically challenging conditions, for example in long-term oxygen minimum zones in the SE-Pacific, tropical E-Atlantic and N-Indian Ocean (Levin et al., 2009). In some of these areas, higher faunal biomasses have been observed at the lower boundary of the OMZ, partially explained by higher food availability (Mosch et al., 2012). Furthermore,

the thresholds for faunal activity can reach much lower oxygen concentrations than in regions, which are facing periodic hypoxia (Levin et al., 2009, Levin 2003). Also in the outer Western Crimean Shelf area, the overall reduction of BMU from the oxic zone to the oxic-hypoxic zone relates well with changes in some macrobenthos composition. In the oxic zone the higher fauna-mediated uptake was probably partly caused by irrigation and bioturbation by polychaetes, bivalves, and gastropods (Table S1). Ventilation of the upper sediment layer is indicated by the presence of oxidized Fe and Mn solid phase minerals in the oxic zone and in the upper 10 cm of the oxic-hypoxic zone (Fig. 7). Decreased bioturbation in the other zones is due to reduced abundances of sediment infauna. Loss of sediment ventilation also explains changes in sediment biogeochemistry, in particular the ceasing of the iron and manganese cycle upon lower bottom-water oxygen concentrations (Fig. 7). In contrast, oxidized forms of iron and manganese are abundant in the surface sediments of the oxic zone. This is in accordance with previous studies that have shown that reoxidation of reduced iron and manganese is mainly stimulated by bioturbation, and thus recycling efficiency of the metals primarily depends on bottom-water oxygen levels and rates of bioturbation (Canfield et al., 1993b; Thamdrup et al., 2000; Wijsman et al., 2001).

The restriction of bivalves and gastropods to the upper oxic-hypoxic zone is surprising, as representatives of these groups are known to be able to maintain their respiration rate at hypoxic oxygen concentrations (Bayne, 1971; Taylor and Brand, 1975). Oxygen concentrations on the outer Western Crimean Shelf (Fig. 2) were mostly well above reported oxygen thresholds, e.g., 50 μmol L^{-1} for bivalves and 25 μmol L^{-1} for gastropods (Keeling et al., 2010; Vaquer-Sunyer and Duarte, 2008). While mollusc distribution indicated low hypoxia-tolerance for the species found in the area, fish were observed in the hypoxic-anoxic zone at oxygen concentrations as low as <20 μmol L^{-1}, which although beyond previously-reported tolerance thresholds (Gray et al., 2002; Pihl et al., 1991; Vaquer-Sunyer and Duarte, 2008), is consistent with the adaptations of some fish species of the Black Sea (Silkin and Silkina, 2005).

The overall role of meiobenthos in oxygen consumption is difficult to assess as it can add to both BMU and DOU by bio-irrigating the sediment as well as enhancing diffusional fluxes (Aller and Aller, 1992; Berg et al., 2001; Rysgaard et al., 2000; Wenzhöfer et al., 2002). Altogether, different distribution patterns were found for meiofauna as compared to macrofauna. Meiobenthos abundances were similar in the oxic and oxic-hypoxic zone, and only sharply decreased in the hypoxic-anoxic zone. As shown previously (Levin et al., 2009)

nematodes and foraminifera dominate meiofauna in hypoxic zones due to their ability to adapt to low oxygen concentrations. In particular, nematodes are known to tolerate hypoxic, suboxic, anoxic or even sulfidic conditions (Sergeeva et al., 2012; Sergeeva and Zaika, 2013; Steyaert et al., 2007; Van Gaever et al., 2006). Some meiobenthos species are known to occur under hypoxic conditions (Sergeeva and Anikeeva, 2014; Sergeeva et al., 2013). The relatively high abundance of apparently living foraminifera in the hypoxic zone might be related to the ability of some species to respire nitrate under anoxic conditions (Risgaard-Petersen et al., 2006).

Regarding the validation of the traditionally-used hypoxia threshold for impact on fauna (63 μmol O_2 L^{-1}, e.g., Diaz, 2001), our results support previous studies where significant changes in community structure were reported already at the onset of hypoxia (Gray et al., 2002; Steckbauer et al., 2011; Vaquer-Sunyer and Duarte, 2008). Our results indicate that fauna-mediated oxygen uptake and biogeochemical fluxes are strongly reduced already at periodical hypoxic conditions, as caused by transport of low-oxygen waters via internal waves or eddies close to the shelf break.

5. Conclusions

This study assesses the effect of different ranges of bottom-water oxygenation and its local fluctuations on carbon remineralization rates, the proportion of microbial vs. fauna-mediated respiration, benthic community structure and the share of anaerobic vs. aerobic microbial respiration pathways. We could show that fauna-mediated oxygen uptake and biogeochemical fluxes can be strongly reduced already at periodically hypoxic conditions around 63 μmol L^{-1}. The diffusive respiration by microbes and small metazoa decreased substantially only when oxygen concentration dropped below 20 μmol L^{-1}. The oxidation of upward diffusing reduced compounds from pore water only played a minor role in the diffusive uptake of oxygen by the sediment, in contrast to previous studies of shelf and upper margin sediments. Hypoxia leads to a substantial decrease of the efficiency of carbon degradation compared to persistently oxygenated zones, where nearly all of the deposited carbon is rapidly mineralized by aerobic respiration. Consequently, already at the onset of hypoxia, or under fluctuating conditions such as caused by internal waves or eddies, substantial amounts of organic matter can accumulate in marine sediments, and ecosystem functioning could be impacted over much larger areas adjacent to hypoxic ecosystems.

Acknowledgements

We thank the Captain and shipboard crew of the RV Maria S. Merian, the JAGO team (GEOMAR, Kiel) and shipboard scientists of the cruise MSM 15/1 for their excellent work at sea. We are grateful for technical assistance from Rafael Stiens, Martina Alisch, Erika Weiz, and Kirsten Neumann. We thank the Sea-Tech technicians of the HGF MPG Joint Research Group for Deep-Sea Ecology and Technology (MPI-AWI) for the construction and maintenance of the in situ devices and the technicians of the Microsensor Group for the construction of microsensors. We thank Tim Ferdelman and Gail Lee Arnold for help with the sediment accumulation rate measurements. The associate editor Jack B. M. Middelburg and three anonymous reviewers are acknowledged for providing valuable comments to the manuscript. This project was financed by the EU 7th FP project HYPOX (*In situ monitoring of oxygen depletion in hypoxic ecosystems of coastal and open seas, and land-locked water bodies*) EC Grant 226213.

References

Abril, G., Commarieu, M.-V., Etcheber, H., Deborde, J., Deflandre, B., Živađinović, M. K., Chaillou, G., and Anschutz, P.: In vitro simulation of oxic/suboxic diagenesis in an estuarine fluid mud subjected to redox oscillations, Estuarine, Coastal and Shelf Science, 88, 279-291, 2010.

Aller, R. and Aller, J.: Meiofauna and solute transport in marine muds, Limnology and Oceanography 37, 1018-1033, 1992.

Archer, D. and Devol, A.: Benthic oxygen fluxes on the Washington shelf and slope: A comparison of in situ microelectrode and chamber flux measurements, Limnology and Oceanography, 37, 614-629, 1992.

Baird, D., Christian, R. R., Peterson, C. H., and Johnson, G. A.: Consequences of hypoxia on estuarine ecosystem function: energy diversion from consumers to microbes, Ecological Applications, 14, 805-822, 2004.

Bayne, B. L.: Oxygen consumption by three species of lamellibranch mollusc in declining ambient oxygen tension, Comparative Biochemistry and Physiology Part A: Physiology, 40, 955-970, 1971.

Berg, P., Risgaard-Petersen, N., and Rysgaard, S.: Interpretation of measured concentration profiles in sediment pore water, Limnology and Oceanography, 43, 1500-1510, 1998.

Berg, P., Rysgaard, S., Funch, P., and Sejr, M.: Effects of bioturbation on solutes and solids in marine sediments, Aquatic Microbial Ecology 26, 81-94, 2001.

Boesch, D. F. and Rabalais, N. N.: Effects of hypoxia on continental shelf benthos: comparisons between the New York Bight and the Northern Gulf of Mexico, in: Modern and Ancient Continental Shelf Anoxia, edited by: Tyson, R. V. and Pearson, T. H., Geological Society Special Publication 58, 27-34, Geological Soc., London, 1991.

Boetius, A. and Wenzhöfer, F.: In situ technologies for studying deep-sea hotspot ecosystems, Oceanography, 22, p 177, doi: 10.5670/oceanog.2009.17, 2009.

Broecker, W. S. and Peng, T. H.: Gas exchange rates between air and sea, Tellus, 26, 21-35, 1974.

Canfield, D. E., Jørgensen, B. B., Fossing, H., Glud, R., Gundersen, J., Ramsing, N. B., Thamdrup, B., Hansen, J. W., Nielsen, L. P., and Hall, P. O. J.: Pathways of organic carbon oxidation in three continental margin sediments, Marine Geology, 113, 27-40, 1993a.

Canfield, D. E., Thamdrup, B., and Hansen, J. W.: The anaerobic degradation of organic matter in Danish coastal sediments: Iron reduction, manganese reduction, and sulfate reduction, Geochim Cosmochim Ac, 57, 3867-3883, 1993b.

Clarke, K.-R.: Non‐parametric multivariate analyses of changes in community structure, Australian Journal of Ecology, 18, 117-143, 1993.

Cline, J. D.: Spectrophotometric determination of hydrogen sulfide in natural waters, Limnology and Oceanography, 14, 454-458, 1969.

Cook, P. L. M., Wenzhöfer, F., Glud, R. N., Janssen, F., and Huettel, M.: Benthic solute exchange and carbon mineralization in two shallow subtidal sandy sediments: Effect of advective pore-water exchange, Limnology and Oceanography 1943-1963, 2007.

Dale, A. W., Bertics, V. J., Treude, T., Sommer, S., and Wallmann, K.: Modeling benthic–pelagic nutrient exchange processes and porewater distributions in a seasonally hypoxic sediment: evidence for massive phosphate release by Beggiatoa?, Biogeosciences, 10, 629-651, 2013.

de Beer, D., Glud, A., Epping, E., and Kuhl, M.: A fast-responding CO_2 microelectrode for profiling sediments, microbial mats, and biofilms, Limnology and Oceanography, 42, 1590-1600, 1997.

Diaz, R. J.: Overview of hypoxia around the world, Journal of Environmental Quality, 30, 275-281, 2001.

Fossing, H. and Jørgensen, B. B.: Measurement of bacterial sulfate reduction in sediments: evaluation of a single-step chromium reduction method, Biogeochemistry, 8, 205-222, 1989.

Friedl, G., Dinkel, C., and Wehrli, B.: Benthic fluxes of nutrients in the northwestern Black Sea, Marine Chemistry, 62, 77-88, 1998.

Friedrich, J., Janssen, F., Aleynik, D., Bange, H. W., Boltacheva, N., Çagatay, M. N., Dale, A. W., Etiope, G., Erdem, Z., Geraga, M., Gilli, A., Gomoiu, M. T., Hall, P. O. J.,

Hansson, D., He, Y., Holtappels, M., Kirf, M. K., Kononets, M., Konovalov, S., Lichtschlag, A., Livingstone, D. M., Marinaro, G., Mazlumyan, S., Naeher, S., North, R. P., Papatheodorou, G., Pfannkuche, O., Prien, R., Rehder, G., Schubert, C. J., Soltwedel, T., Sommer, S., Stahl, H., Stanev, E. V., Teaca, A., Tengberg, A., Waldmann, C., Wehrli, B., and Wenzhöfer, F.: Investigating hypoxia in aquatic environments: diverse approaches to addressing a complex phenomenon, Biogeosciences, 11, 1215-1259, 2014.

Glud, R. N.: Oxygen dynamics of marine sediments, Marine Biology Research, 4, 243–289, 2008.

Glud, R. N., Gundersen, J. K., Røy, H., and Jørgensen, B. B.: Seasonal dynamics of benthic O_2 uptake in a semi-enclosed bay: Importance of diffusion and faunal activity, Limnology and Oceanography, 48, 1265-1276, 2003.

Glud, R. N., Holby, O., Hoffmann, F., and Canfield, D. E.: Benthic mineralization and exchange in Arctic sediments (Svalbard, Norway), Marine Ecology Progress Series, 173, 237-251, 1998.

Grasshoff, K.: Methods of seawater analysis, Verlag Chemie, Weinheim, 1983.

Gray, J. S., Wu, R. S.-s., and Or, Y. Y.: Effects of hypoxia and organic enrichment on the coastal marine environment, Marine Ecology Progress Series, 238, 249–279, 2002.

Grego, M., Stachowitsch, M., De Troch, M., and Riedel, B.: CellTracker Green labelling vs. rose bengal staining: CTG wins by points in distinguishing living from dead anoxia-impacted copepods and nematodes, Biogeosciences, 10, 4565-4575, 2013.

Grégoire, M. and Friedrich, J.: Nitrogen budget of the north-western Black Sea shelf as inferred from modeling studies and in-situ benthic measurements, Marine Ecology Progress Series, 270, 15-39, 2004.

Heip, C. H. R., Duineveld, G., Flach, E., Graf, G., Helder, W., Herman, P. M. J., Lavaleye, M., Middelburg, J. J., Pfannkuche, O., Soetaert, K., Soltwedel, T., de Stigter, H., Thomsen, L., Vanaverbeke, J., and de Wilde, P.: The role of the benthic biota in sedimentary metabolism and sediment-water exchange processes in the Goban Spur area (NE Atlantic), Deep Sea Research Part II: Topical Studies in Oceanography, 48, 3223-3243, 2001.

Heip, C. H. R., Goosen, N. K., Herman, P. M. J., Kromkamp, J., Middelburg, J. J., and Soetaer, K.: Production and consumption of biological particles in temperate tidal estuaries, Ann. Rev. Ocean. Mar. Biol, 33, 1–150, 1995.

Holtappels, M., Glud, R. N., Donis, D., Liu, B., Hume, A., Wenzhöfer, F., and Kuypers, M. M. M.: Effects of transient bottom water currents and oxygen concentrations on benthic exchange rates as assessed by eddy correlation measurements, Journal of Geophysical Research: Oceans, 118, 1157-1169, 2013.

Holtappels, M., Kuypers, M. M., Schlüter, M., and Brüchert, V.: Measurement and interpretation of solute concentration gradients in the benthic boundary layer, Limnology and Oceanography: Methods, 9, 1-13, 2011.

Jahnke, R. A., Reimers, C. E., and Craven, D. B.: Intensification of recycling of organic matter at the sea floor near ocean margins, Nature, 348, 50-54, 1990.

Jeroschewski, P., Steuckart, C., and Kühl, M.: An amperometric microsensor for the determination of H_2S in aquatic environments, Analytical Chemistry, 68, 4351-4357, 1996.

Jørgensen, B. B.: A comparison of methods for the quantification of bacterial sulfate reduction in coastal marine sediments, Geomicrobiology Journal, 1, 11-27, 1978.

Jørgensen, B. B.: Mineralization of organic matter in the sea bed—the role of sulphate reduction, Nature, 643-645, 1982.

Kallmeyer, J., Ferdelman, T. G., Weber, A., Fossing, H., and Jørgensen, B. B.: A cold chromium distillation procedure for radiolabeled sulfide applied to sulfate reduction measurements, Limnology and Oceanography: Methods, 2, 171-180, 2004.

Keeling, R. F., Kortzinger, A., and Gruber, N.: Ocean deoxygenation in a warming world, Annual Review of Marine Science 2, 199-229 2010.

King, L. L.: A mass balance of chlorophyll degradation product accumulation in Black Sea sediments, Deep Sea Research Part I: Oceanographic Research Papers 42, 919-942, 1995.

Konovalov, S. K., Luther III, G. W., and Yücel, M.: Porewater redox species and processes in the Black Sea sediments, Chemical Geology, 245, 254-274, 2007.

Levin, L. A.: Oxygen minimum zone benthos: adaptation and community response to hypoxia, Oceanogr. Mar. Biol. Ann. Rev., 41, 1–45, 2003.

Levin, L. A., Ekau, W., Gooday, A. J., Jorissen, F., Middelburg, J. J., Naqvi, W., Neira, C., Rabalais, N. N., and Zhang, J.: Effects of natural and human-induced hypoxia on coastal benthos, Biogeosciences, 6, 3563-3654, 2009.

Lichtschlag, A., Felden, J., Wenzhöfer, F., Schubotz, F., Ertefai, T. F., Boetius, A., and de Beer, D.: Methane and sulfide fluxes in permanent anoxia: In situ studies at the Dvurechenskii mud volcano (Sorokin Trough, Black Sea), Geochim Cosmochim Ac, 74, 5002-5018, 2010.

Luth, U., Luth, C., Stokozov, N. A. and Gulin, M. B.: The chemocline rise effect on the northwestern slope of the Black Sea, in: Methane Gas Seep Explorations in the Black Sea (MEGASEEBS), Project Report. Ber. Zentrum Meeres- u. Klimaforsch., edited by: Luth, U., Luth, C., and Thiel, H., Univ. Hamburg, Reihe E, 14, 59–77, 1998.

Middelburg, J. J., Levin, L. A.: Coastal hypoxia and sediment biogeochemistry, Biogeosciences, 6, 1273-1293, 2009.

Moodley, L., Schaub, B. E. M., Zwaan, G. J. v. d., and Herman, P. M. J.: Tolerance of benthic foraminifera (Protista: Sarcodina) to hydrogen sulphide, Ecology Progress Series, 169, 77-86, 1998.

Mosch, T., Sommer, S., Dengler, M., Noffke, A., Bohlen, L., Pfannkuche, O. Liebetraut, V. and Wallmann, K.: Factors influencing the distribution of epibenthic megafauna across the Peruvian oxygen minimum zone. Deep Sea Research Part I: Oceanographic Research Papers, 68, 123-135, 2012.

Murray, J. W. and Yakushev, E.: The suboxic transition zone in the Black Sea, in: Past and Present Marine Water Column Anoxia, edited by: Neretin, L., NATO Science Series IV: Earth and Environmental Sciences, 64, Springer, Dordrecht, 105-138, doi:10.1007/1-4020-4297-3_05,2006.

Niggemann, J., Ferdelman, T. G., Lomstein, B. A., Kallmeyer, J., and Schubert, C. J.: How depositional conditions control input, composition, and degradation of organic matter in sediments from the Chilean coastal upwelling region, Geochim Cosmochim Ac, 71, 1513-1527, 2007.

Oksanen, J., Blanchet, F. G., Kindt, R., Legendre, P., Minchin, P. R., O'Hara, R. B., Simpson, G. L., Solymos, P., Stevens, M. H. H., Wagner, H.: vegan: Community Ecology Package, R package version of The Comprehensive R Archive Network, 1.17-3, 2010.

Pearson, T. H. and Rosenberg, R.: Energy flow through the SE Kattegat: A comparative examination of the eutrophication of a coastal marine ecosystem, Netherlands Journal of Sea Research, 28, 317-334, 1992.

Piepenburg, D., Blackburn, H., T., Dorrien, v., F., C., Gutt, J., Hall, J., P. O., Hulth, S., Kendall, A., M., Opalinski, W., K., Rachor, E., Schmid, and K., M.: Partitioning of benthic community respiration in the Arctic (northwestern Barents Sea), Marine Ecology Progress Series, 118, 199-213, 1995.

Pihl, L., Baden, S. P., and Diaz, R. J.: Effects of periodic hypoxia on distribution of demersal fish and crustaceans, Mar. Biol., 108, 349-360, 1991.

Poulton, S. W. and Canfield, D. E.: Development of a sequential extraction procedure for iron: implications for iron partitioning in continentally derived particulates, Chemical Geology, 214, 209-221, 2005.

Rasmussen, H. and Jørgensen, B. B.: Microelectrode studies of seasonal oxygen uptake in a coastal sediment: role of molecular diffusion, Marine Ecology Progress Series 81, 289-303, 1992.

Revsbech, N. P.: An oxygen microsensor with a guard cathode, Limnol. Oceanogr., 34, 474-478, doi: 10.4319/lo.1989.34.2.0474, 1989.

Risgaard-Petersen, N., Langezaal, A. M., Ingvardsen, S., Schmid, M. C., Jetten, M. S. M., Op den Camp, H. J. M., Derksen, J. W. M., Pina-Ochoa, E., Eriksson, S. P., Peter Nielsen, L., Revsbech, N. P., Cedhagen, T., and van der Zwaan, G. J.: Evidence for complete denitrification in a benthic foraminifera, Nature, 443, 93-96, 2006.

Rossi, F., Gribsholt, B., Middelburg, J. J., and Heip, C.: Context-dependent effects of suspension feeding on intertidal ecosystem functioning, Marine Ecology Progress Series, 354, 47-57, 2008.

Rysgaard, S., Christensen, P., Sørensen, M., Funch, P., and Berg, P.: Marine meiofauna, carbon and nitrogen mineralization in sandy and soft sediments of Disko Bay, West Greenland, Aquatic Microbial Ecology 21, 59-71, 2000.

Seeberg-Elverfeldt J., Schlüter M., Feseker T. and Kolling M.: Rhizon sampling of porewaters near the sediment–water interface of aquatic systems. Limnology and Oceanography: Methods, 3, 361–371, 2005.

Sergeeva, N., Gooday, A. J., Mazlumyan, S. A., Kolesnikova, E. A., Lichtschlag, A., Koshelva, T. N., and Anikeeva, O. V.: Meiobenthos of the oxic/anoxic interface in the southwestern region of the Black Sea: abundance and taxonomic composition, in: ANOXIA: Evidence for Eukaryote Survival and Paleontological Strategies, edited by: Altenbach, A. V., Bernhard, J. M., and Seckbach, J., Cellular Origin, Life in Extreme Habitats and Astrobiology, 21, Springer, Dordrecht, 369-401, doi: 10.1007/978-94-007-1896-8_20, 2012.

Sergeeva, N. G. and Anikeeva, O. V.: Soft-walled foraminifera under normoxia/hypoxia conditions in the shallow areas of the Black Sea, in: Foraminifera. Aspects of Classification, Stratigraphy, Ecology and Evolution, edited by: Georgescu, M. D., Nova Publ., New York, 227-247, 2014.

Sergeeva, N. G., Mazlumyan, S. A., Çağatay, N., and Lichtschlag, A.: Hypoxic meiobenthic communities of the Istanbul Strait's (Bosporus) outlet area of the Black Sea, Turkish Journal of Fisheries and Aquatic Sciences, 13, 33-41, 2013.

Sergeeva, N. G. and Zaika, V. E.: The Black Sea meiobenthos in permanently hypoxic habitat, Acta zoologica bulgarica, 65 139-150, 2013.

Silkin, Y. A. and Silkina, E. N.: Effect of hypoxia on physiological-biochemical blood parameters in some marine fish, J Evol Biochem Phys, 41, 527-532, 2005.

Soetaert, K., Herman, P. M. J., and Middelburg, J. J.: A model of early diagenetic processes from the shelf to abyssal depths, Geochim Cosmochim Ac, 60, 1019-1040, 1996.

Stanev, E. V., Beckers, J. M., Lancelot, C., Staneva, J. V., Le Traon, P. Y., Peneva, E. L., and Gregoire, M.: Coastal–open ocean exchange in the Black Sea: observations and modelling, Estuarine, Coastal and Shelf Science, 54, 601-620, 2002.

Stanev, E. V., He, Y., Grayek, S., and Boetius, A.: Oxygen dynamics in the Black Sea as seen by Argo profiling floats, Geophys. Res. Lett., 40, 3085-3090, 2013.

Staneva, J. V., Dietrich, D. E., Stanev, E. V., and Bowman, M. J.: Rim current and coastal eddy mechanisms in an eddy-resolving Black Sea general circulation model, Journal of Marine Systems, 31, 137-157, 2001.

Steckbauer, A., Duarte, C. M., Carstensen, J., Vaquer-Sunyer, R., and Conley, D. J.: Ecosystem impacts of hypoxia: thresholds of hypoxia and pathways to recovery, Environ. Res. Lett., 6, 025003 (12pp), doi: 10.1088/1748-9326/6/2/025003, 2011.

Steyaert, M., Moodley, L., Nadong, T., Moens, T., Soetaert, K., and Vincx, M.: Responses of intertidal nematodes to short-term anoxic events, Journal of Experimental Marine Biology and Ecology, 345, 175-184, 2007.

Taylor, A. C. and Brand, A. R.: A comparative study of the respiratory responses of the bivalves Arctica islandica (L.) and Mytilus edulis L. to declining oxygen tension, Proceedings of the Royal Society of London. Series B. Biological Sciences, 190, 443-456, 1975.

Thamdrup, B., Rosselló-Mora, R., and Amann, R.: Microbial manganese and sulfate reduction in Black Sea shelf sediments, Applied and Environmental Microbiology 66, 2888–2897, 2000.

Tolmazin, D.: Changing coastal oceanography of the Black Sea. I: Northwestern shelf, Progress in Oceanography, 15, 217-276, 1985.

Van Gaever, S., Moodley, L., de Beer, D., and Vanreusel, A.: Meiobenthos at the Arctic Håkon Mosby Mud Volcano, with a parental-caring nematode thriving in sulphide-rich sediments, Marine Ecology Progress Series, 321, 143-155, 2006.

Vandewiele, S., Cowie, G., Soetaert, K., and Middelburg, J. J.. Amino acid biogeochemistry and organic matter degradation state across the Pakistan margin oxygen minimum zone. Deep Sea Research Part II: Topical Studies in Oceanography, 56, 376-392, 2009.

Vaquer-Sunyer, R., C. M. Duarte: Thresholds of hypoxia for marine biodiversity, Proceedings of the National Acadamy of Sciences of the United States of America, 105, 15452–15457, 2008.

Waldmann, C. and Bergenthal, M.: CMOVE – a versatile underwater vehicle for seafloor studies, OCEANS 2010 Proc., IEEE conference, 20-23 September, Seattle, WA, USA, doi:2010,10.1109/OCEANS.2010.5664261, 2010.

Weber, A., Riess, W., Wenzhoefer, F., and Jørgensen, B. B.: Sulfate reduction in Black Sea sediments: in situ and laboratory radiotracer measurements from the shelf to 2000m depth, Deep Sea Research Part I: Oceanographic Research Papers, 48, 2073-2096, 2001.

Wenzhöfer, F. and Glud, R. N.: Benthic carbon mineralization in the Atlantic: a synthesis based on in situ data from the last decade, Deep Sea Research Part I: Oceanographic Research Papers, 49, 1255-1279, 2002.

Wenzhöfer, F. and Glud, R. N.: Small-scale spatial and temporal variability in coastal benthic O_2 dynamics: Effects of fauna activity, Limnology and Oceanography, 49, 1471-1481, 2004.

Wenzhöfer, F., Riess, W., and Luth, U.: In situ macrofaunal respiration rates and their importance for benthic carbon mineralization on the northwestern Black Sea shelf, Ophelia, 56, 87-100, 2002.

Wijsman, J. W. M., Middelburg, J. J., and Heip, C. H. R.: Reactive iron in Black Sea sediments: Implications for iron cycling, Mar Geol, 172, 167-180, 2001.

Winkler, L.: The determination of dissolved oxygen in water, Ber Dtsch Chem Ges 21, 2843–2857, 1888.

Witte, U. and Pfannkuche, O.: High rates of benthic carbon remineralisation in the abyssal Arabian Sea, Deep Sea Research Part II: Topical Studies in Oceanography, 47, 2785-2804, 2000.

Zaika, V. E. and Gulin, M. B.: The maximum depths of fish inhabitation in the Black Sea and features of their trophic strategy nearly of oxic/anoxic interface, Marine Ecology Journal, 10, 39 – 47, (in Russian), 2011.

Zaika, V. E., Konovalov, S. K., and Sergeeva., N.: The events of local and seasonal hypoxia at the bottom of Sevastopol bays and their influence on macrobenthos, Marine Ecology Journal, 10, 15-25, 2011.

Zopfi, J., Ferdelman, T. G., and Fossing, H.: Distribution and fate of sulfur intermediates – sulfite tetrathionate, thiosulfate, and elemental sulfur – in marine sediments, in: The Biogeochemistry of Sulfur, GSA Special Paper, edited by: Amend, J., Edwards, K., and Lyons, T., Geol. Soc. America, London, 97-116, 2004.

Table 1. Measurements and samples (including PANGAEA event labels) taken in zones with different oxygen regime. PUC = JAGO pushcores, MOVE = benthic crawler move (in situ microsensor measurements and /or benthic chamber deployment), TVMUC = video-guided multicorer, KAMM = lander (in situ microsensor measurements and /or benthic chamber deployment).

Zone	Water depth (m)	Station/PANGAEA event label	Position	Date	Device	Method
oxic zone <130m bottom-water oxygen conc. > 63 µmol L^{-1}	101	MSM15/1_482_ PUC 1, 3, 5, 6	44° 49.00' N 33° 09.37' E	03.05.2010	PUC	Macro- and meiobenthos
	104	MSM15/1_484-1	44° 49.49' N 33° 09.32' E	03.05.2010	MOVE	Benthic oxygen uptake
	104	MSM15/1_464-1	44° 49.45' N 33° 09.26' E	02.05.2010	TVMUC	Macro- and meiobenthos
	104	MSM15/1_462-1	44° 49.45' N 33° 09.26' E	02.05.2010	TVMUC	Geochemistry
	106	MSM15/1_469-1	44° 49.46' N 33° 09.67' E	02.05.2010	KAMM	Benthic oxygen uptake
	105	MSM15/1_444_ PUC 1	44° 49.32' N 33° 09.46' E	01.05.2010	PUC	Macro- and meiobenthos
	117	MSM15/1_440 _PUC 5, 6	44° 40.49' N 33° 05.53' E	01.05.2010	PUC	Macro- and meiobenthos
	120	MSM15/1_459-1, 2	44° 40.48' N 33° 05.53' E	02.05.2010	TVMUC	Macro- and meiobenthos
	129	MSM15/1_486_ PUC 1, 7	44° 39.13' N 33° 01.78' E	04.05.2010	PUC	Macro- and meiobenthos
oxic-hypoxic (130-142 m) bottom-water oxygen conc. > 63 to > 0 µmol L^{-1}	131	MSM15/1_460 _PUC-1	44° 39.26' N 33° 01.12' E	02.05.2010	PUC	Macro- and meiobenthos
	136	MSM15/1_487-1	44° 38.78' N 33° 00.25' E	04.05.2010	TVMUC	Geochemistry
	137	MSM15/1_434-1	44° 38.93' N 32° 59.98' E	01.05.2010	KAMM	Benthic oxygen uptake
	137	MSM15/1_455-1	44° 38.92' N 32° 59.97' E	02.05.2010	MOVE	Benthic oxygen uptake
	138	MSM15/1_489- 1, 2	44° 38.79' N 33° 00.25' E	04.05.2010	TVMUC	Macro- and meiobenthos
	140	MSM15/1_499-1	44° 38.80' N 33° 00.26' E	05.05.2010	KAMM	Benthic oxygen uptake
hypoxic-anoxic (142-167 m) bottom-water oxygen conc. 63-0 µmol L^{-1}	145	MSM15/1_512-3	44° 37.39' N 32° 56.21' E	05.05.2010	PUC	Macro- and meiobenthos
	151	MSM15/1_372_ PUC 1	44° 37.46' N 32° 54. 91'E	25.04.2010	PUC	Macro- and meiobenthos
	154	MSM15/1_383-1	44° 37.74' N 32° 54.92' E	26.04.2010	KAMM	Benthic oxygen uptake
	155	MSM15/1_379-1	44° 37.55' N 32° 54.97' E	26.04.2010	TVMUC	Macro- and meiobenthos
	156	MSM15/1_386-1	44° 37.58' N 32° 54.97' E	26.04.2010	MOVE	Benthic oxygen uptake
	162	MSM15/1_374-1	44° 37.07' N 32° 53.49' E	25.04.2010	PUC	Macro- and meiobenthos
	163	MSM15/1_425-1	44° 47.09' N 31° 58.05' E	30.04.2010	TVMUC	Macro- and meiobenthos
	164	MSM15/1_393-1	44° 37.08' N 32° 53.48' E	27.04.2010	TVMUC	Geochemistry
anoxic-sulfidic zone (>167m) sulfide present in anoxic bottom water	207	MSM15/1_448-1	44° 35.84' N 32° 49.03' E	01.05.2010	TVMUC	Geochemistry

Table 2. Diffusive oxygen uptake (DOU) rates, total oxygen uptake (TOU) rates and oxygen penetration depth under different oxygen regimes at the outer Western Crimean Shelf. Chamber measurements in the hypoxic-anoxic zone represent potential rates, scaled to a bottom-water oxygen concentration of 20 µmol O_2 L^{-1} (instead of 70 µmol O_2 L^{-1})**.**

Zone	DOU J_{O2} ±SD (mmol $m^{-2}d^{-1}$)	TOU J_{O2} ±SD (mmol $m^{-2}d^{-1}$)	DOU:TOU ration (%)	Oxygen penetration depth ±SD (mm)	C_{org}±SD (%dw)
oxic zone <130m bottom-water oxygen conc. > 63 µmol L^{-1}	4.6 ±1.8 range: 2.4 to 8.1, n =15	14.9 ±5.1 range: 9 to 20.6, n =5	30:70	5.3 ±2.5	2.7 ±1.0
oxic-hypoxic (130-142 m) bottom-water oxygen conc. > 63 to > 0 µmol L^{-1}	4.4 ±1.9 range: 0.6 to 8.0, n =12	7.3 ±3.5 range: 3.2 to 9.4, n =3	60:40	1.6 ±1.2	4.6 ±0.9
hypoxic-anoxic (142-167 m) bottom water oxygen conc. 63-0 µmol L^{-1}	1.3 ±0.5 range: 0.8 to 2.1, n =5 (potential rate: 5.6)	*1.6 ±0.5 Modeled*	80:20 (*modeled from potential rates*)	0.4 ±0.1	5.8 ±1.7

Table 3. Diffusive oxygen uptake compared to fluxes of reduced species, calculated from the modeled profiles (Fig. 7) or measured directly (SRR = Sulfate reduction rates). The sum in oxygen equivalents is calculated from the stoichiometry of the oxidation processes (respective formulas are displayed at the lower end of the table), and oxygen available for direct aerobic respiration is calculated by subtracting the potential oxygen demand from the available oxygen flux.

	Oxygen flux (mmol m^{-2} d^{-1})	Reduced species fluxes (mmol m^{-2} d^{-1})					
	DOU (J_{O2}) *see Table 2*	J_{Fe}^{2+}	J_{Mn}^{2+}	$J_{sulfide}$ / SRR	J_{NH4}^{+}	SUM in oxygen equivalents	Diffusive oxygen consumption (direct aerobic mineralization : reoxidation) in mmol m^{-2} d^{-1} and %
oxic zone <130m, bottom-water oxygen conc. > 63 µmol L^{-1}	- 4.6	0.1	<0.1	0*/<0.1	0.1	0.23	4.38 : 0.23 95 % : 5 %
oxic-hypoxic 130-142 m, bottom-water oxygen conc. > 63 to > 0 µmol L^{-1}	- 4.4	0.1	0	0*/0.4	<0.1	<0.1	4.36 : <0.1 >98 % :<2 %
hypoxic-anoxic 142-167 m, bottom-water oxygen conc. 63-0 µmol L^{-1}	-1.3	0	0	0*/0.2	<0.1	<0.1	1.3 : <0.1 >92 %: < 8%
anoxic-sulfidic zone >167 m, sulfide present in anoxic bottom water	0	0	0	0.5/3.7	0.1	1.1	0: 1.1** 0 % : 100 %

Negative numbers denote downward flux, positive numbers upward flux

* bottom-water sulfide was zero

** potential oxygen demand is higher than oxygen availability, thus reducing components are emitted

$OM + O_2 \rightarrow CO_2 + H_2O$ ratio 1:1

$H_2S + 2O_2 \rightarrow SO_4^{2-} + 2H^+$ ratio 1:2

$4Fe^{2+} + O_2 + 6H_20 \rightarrow 4FeOOH + 8H^+$ ratio 4:1

$2Mn^{2+} + O_2 + 2H_20 \rightarrow 2MnO_2 + 4H^+$ ratio 2:1

$NH_4^+ + 2O_2 \rightarrow NO_3^- + H_20 + 2H^+$ ratio 1:2

1 Table 4. Oxygen consumption in hypoxic areas of the Black Sea, n.d. = not determined.

2

Area	Water depth (m)	Oxygen concentration (μmol L^{-1})	TOU (mmol m^{-2} d^{-1})	DOU (mmol m^{-2} d^{-1})	Method	Fauna	Reference
Bay of Varna	24	230	33.3		in situ chamber	living organisms	
Danube delta front	26	160	25.9		(TOU)	living organisms	
Danube prodelta	27	0				living organisms	Fridel at al. 1998
shelf edge	134	40	0			no living organisms	
shelf edge	142	30	5.7			living organisms	
Romanian Shelf	62	211	39.8	11.9	in situ chamber	*Mytilus galloprovinciales*	Wenzhöfer et al.
	77	213	11.1	5.8	(TOU)/	*Modiolus phaseolinus*	2002
	100	75	4.3	2.3	microsensors	*Modiolus phaseolinus*	
	180	8	0	0	(DOU)	*no macrofauna*	
NW Shelf	52	285	13.5, 10, 11.6		ex situ core	n.d.	Wijsman et al. 2001
	54	314	11, 6.1		incubations		
	57	243	3.7		(TOU)		
	72	284					
	120	126					
	137	190					
Crimean Shelf	135	95	4.2-6		Eddy correlation		Holtappels et al., 2013
Crimean Shelf	104	110-134	11.6	4.6	in situ chamber	living organisms	this study
	135	18-149	6.7	4.4	(TOU)/	living organisms	
	155	19-11	n.d.	1.3	microsensors	living organisms,	
					(DOU)	including fish	

Fig. 1: Sediment sampling locations (TVMUC = video-guided multicorer, PUC = JAGO pushcores) and deployment sites of benthic chamber and microprofiler with MOVE and lander (KAMM) along the transect from shallower (101 m) to deeper (207 m) water depth. Inset: working area on the outer Western Crimean Shelf (red square) in the Black Sea.

Fig. 2: Synthesis of oxygen concentrations in bottom water (circles) measured during the 2 weeks of the cruise (n=85). For continuously measuring instruments (BBL profiler, optode on JAGO, benthic lander, moorings) only an average value per deployment, dive or day was included. Maximum depth above the sediment was 12 m (CTD), minimum depth above the sediment was about 5 cm (Clark-type oxygen microelectrodes). Additionally, sulfide distribution in bottom waters during the same sampling period are shown (white diamonds, n=43). From depth distribution of oxygen and sulfide the distribution in i) oxic, ii) oxic-hypoxic, iii) hypoxic-anoxic and iv) anoxic-sulfidic zone was deduced.

Fig. 3: Abundance of meiobenthos in the upper five centimeter of the sediment under different oxygen regimes. The middle line in each box depicts the median, while both whiskers and outliers indicate the distribution of remaining data points.

Fig. 4: Cluster dendrogram of meiofauna abundances for different station depths based on the inverse of Bray-Curtis dissimilarity.

Fig. 5: Examples of high-resolution oxygen profiles under different oxygen regimes. Differences in bottom-water oxygen concentrations (reflected in profile shape and oxygen penetration depth) are clearly visible between sites and deployments.

Fig. 6: Examples of individual oxygen profiles measured in the sediment (white circles) and modeled with PROFILER (black lines). Volumetric rates are combined in discrete layers (dashed line) and exhibit different depths and degrees of oxygen consumption rates in different zones and under different bottom-water oxygenation.

Fig. 7: Distribution of reduced pore-water species and oxidized and solid phase iron and sulfur species along the depth transect in the upper 30 cm of the sediment (symbols with dotted lines). Solid lines are the model results and dashed lines represent production and consumption rates.

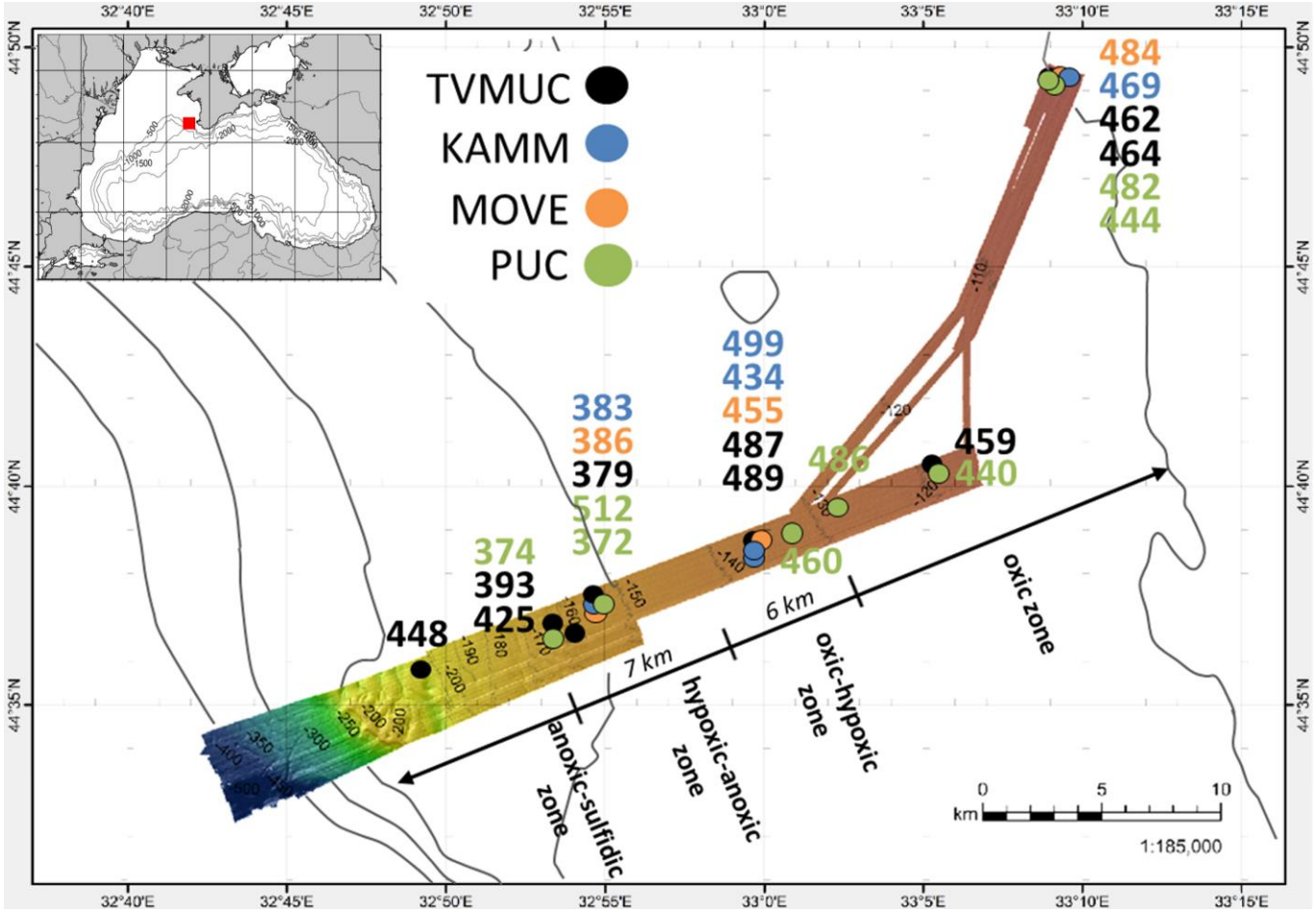
TVMUC
KAMM
MOVE
PUC
484
469
462
464
482
444
499
434
455
487
489
383
386
379
512
372
374
393
425
448
486
459
440
460
7 km
6 km
anoxic-sulfidic zone
hypoxic-anoxic zone
oxic-hypoxic zone
oxic zone
0
5
10
km
1:185,000
32°40'E
32°45'E
32°50'E
32°55'E
33°0'E
33°5'E
33°10'E
33°15'E
44°50'N
44°45'N
44°40'N
44°35'N

Figure 1

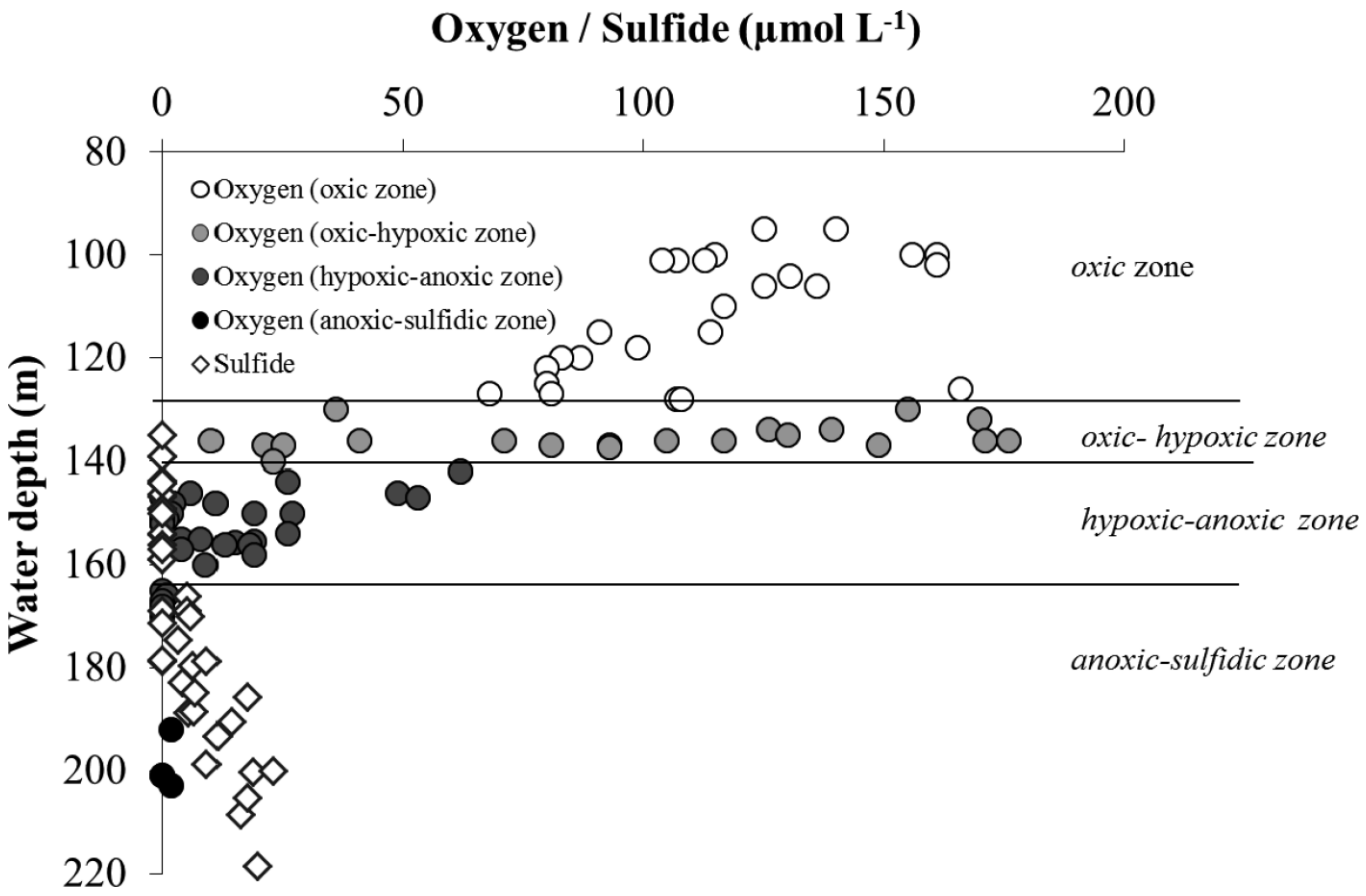
Oxygen / Sulfide (µmol L-1)
0
50
100
150
200
80
100
120
140
160
180
200
220
Water depth (m)
Oxygen (oxic zone)
Oxygen (oxic-hypoxic zone)
Oxygen (hypoxic-anoxic zone)
Oxygen (anoxic-sulfidic zone)
Sulfide
oxic zone
oxic- hypoxic zone
hypoxic-anoxic zone
anoxic-sulfidic zone

Figure 2

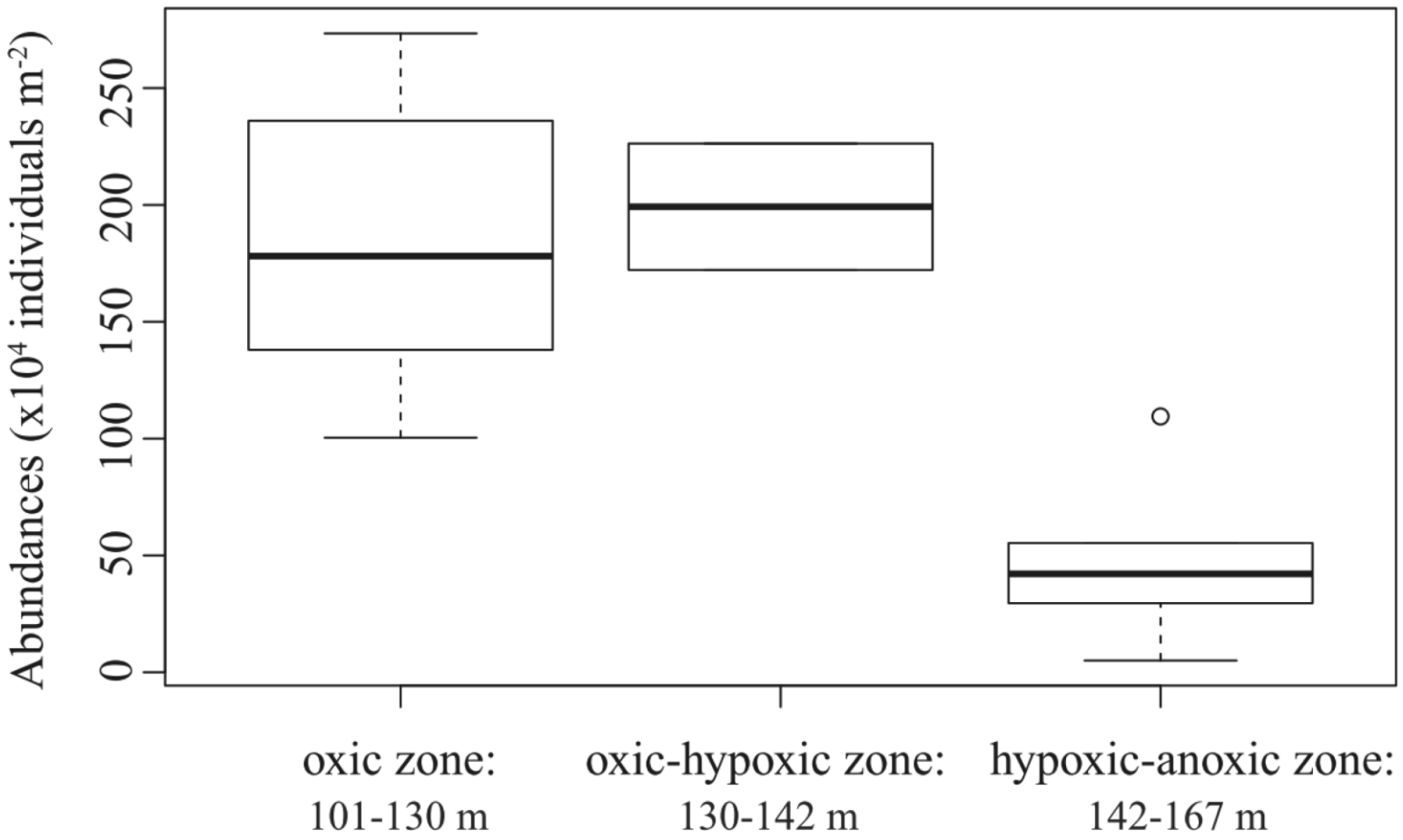
Abundances (x10^4 individuals m^-2)
0
50
100
150
200
250
oxic zone:
101-130 m
oxic-hypoxic zone:
130-142 m
hypoxic-anoxic zone:
142-167 m

Figure 3

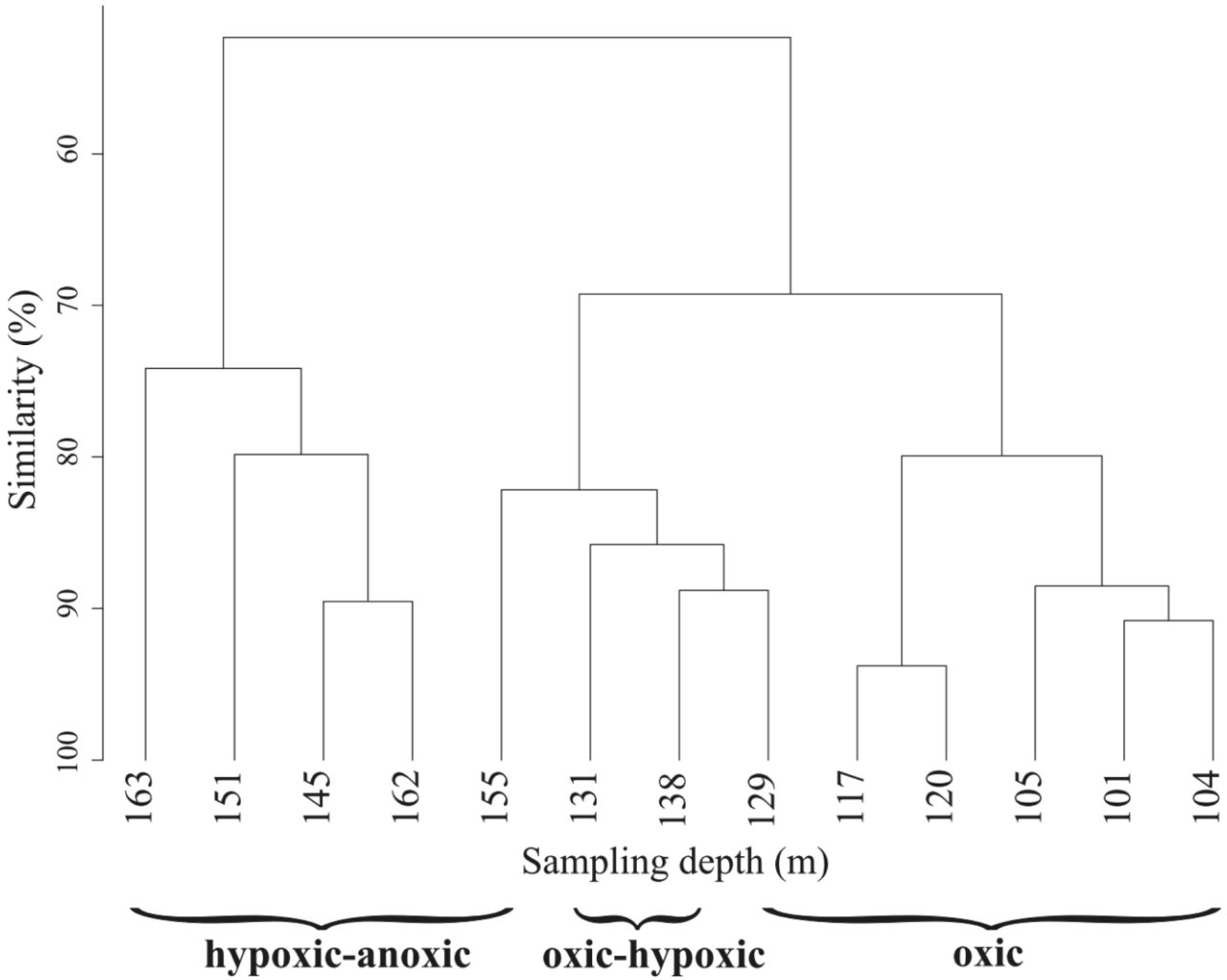
Similarity (%)
100
90
80
70
60
163
151
145
162
155
131
138
129
117
120
105
101
104
Sampling depth (m)
hypoxic-anoxic
oxic-hypoxic
oxic

Figure 4

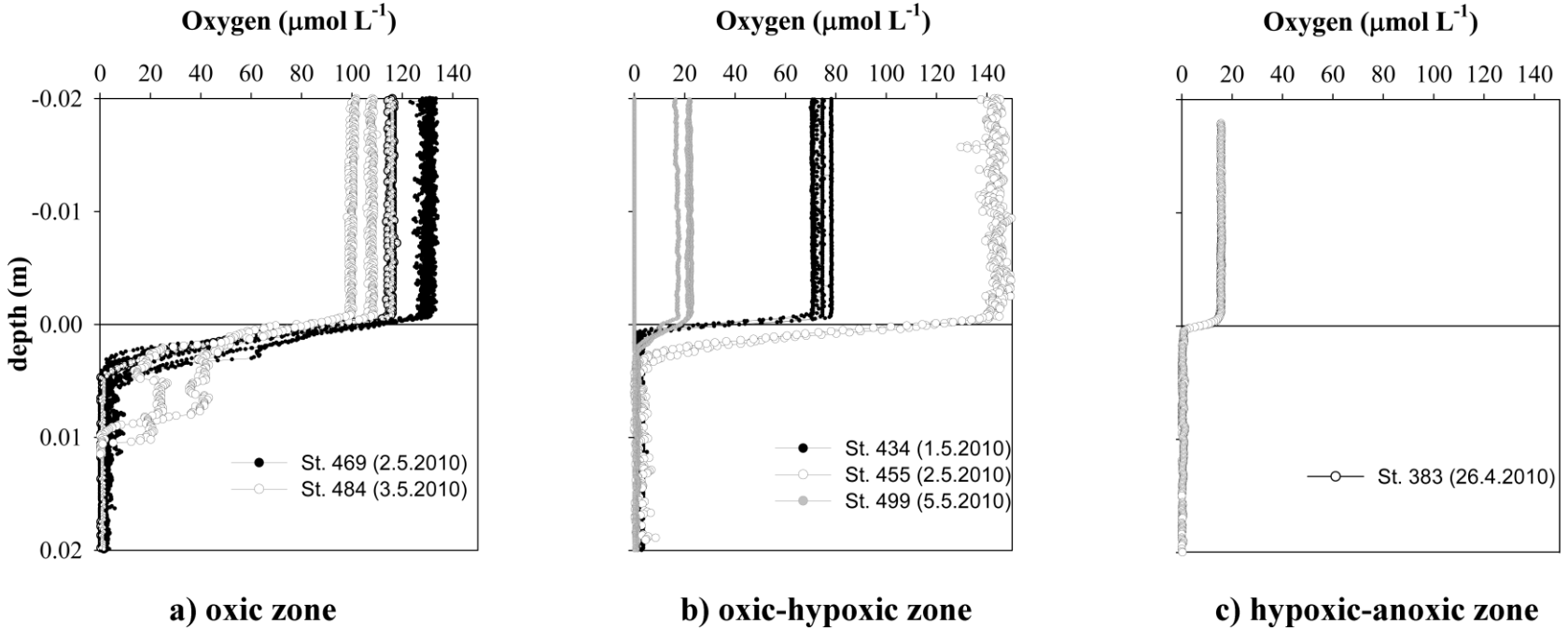
Oxygen (µmol L-1)
0 20 40 60 80 100 120 140
-0.02
-0.01
0.00
0.01
0.02
depth (m)
St. 469 (2.5.2010)
St. 484 (3.5.2010)
a) oxic zone
Oxygen (µmol L-1)
0 20 40 60 80 100 120 140
St. 434 (1.5.2010)
St. 455 (2.5.2010)
St. 499 (5.5.2010)
b) oxic-hypoxic zone
Oxygen (µmol L-1)
0 20 40 60 80 100 120 140
St. 383 (26.4.2010)
c) hypoxic-anoxic zone

Figure 5

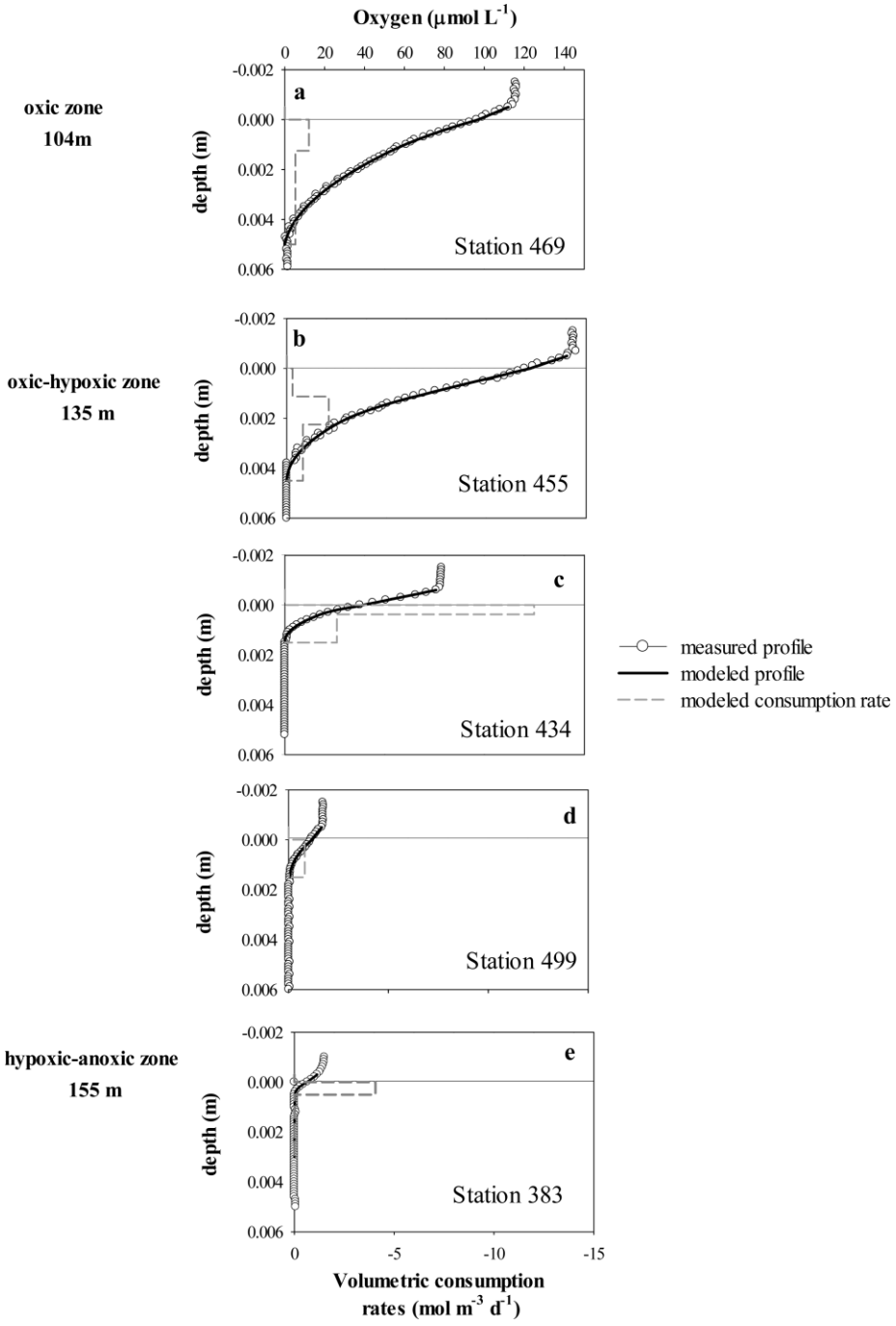
Oxygen (µmol L-1)
0 20 40 60 80 100 120 140
oxic zone
104m
a
Station 469
oxic-hypoxic zone
135 m
b
Station 455
c
Station 434
d
Station 499
hypoxic-anoxic zone
155 m
e
Station 383
depth (m)
-0.002
0.000
0.002
0.004
0.006
0 -5 -10 -15
Volumetric consumption rates (mol m-3 d-1)
measured profile
modeled profile
modeled consumption rate

Figure 6

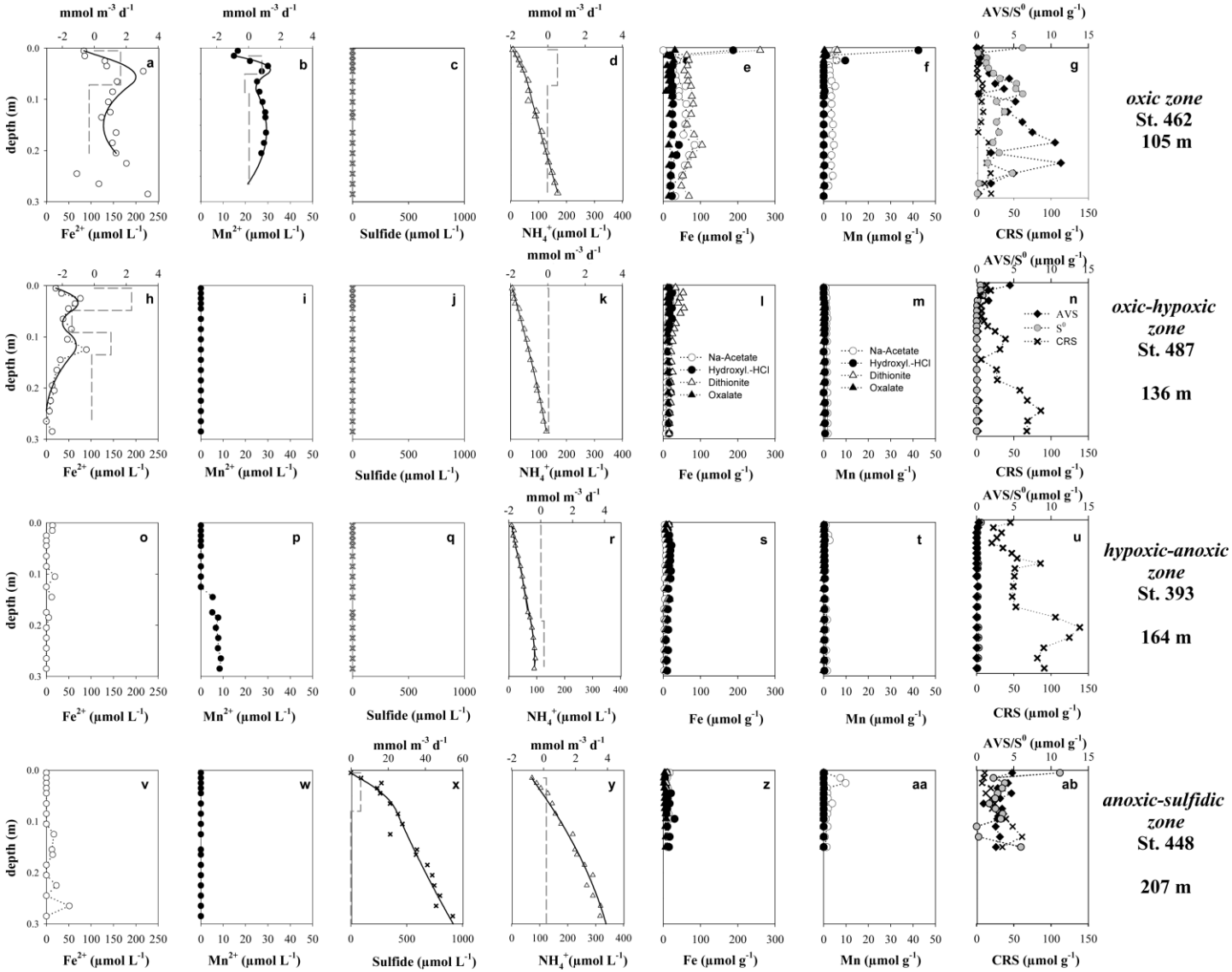
mmol m-3 d-1
AVS/S0 (µmol g-1)
depth (m)
Fe2+ (µmol L-1)
Mn2+ (µmol L-1)
Sulfide (µmol L-1)
NH4+(µmol L-1)
Fe (µmol g-1)
Mn (µmol g-1)
CRS (µmol g-1)
Na-Acetate
Hydroxyl.-HCl
Dithionite
Oxalate
AVS
S0
CRS
oxic zone
St. 462
105 m
oxic-hypoxic zone
St. 487
136 m
hypoxic-anoxic zone
St. 393
164 m
anoxic-sulfidic zone
St. 448
207 m

Figure 7